Petroleum Science 22 (2025) 4895–4909

Contents lists available at ScienceDirect

Petroleum Science

journal homepage: www.keaipublishing.com/en/journals/petroleum-science

Review Paper

Research progress and scientific challenges in permeability evolution of hydrate bearing sediments

Yao-Bin Li [a,b], Xin Xin [a,b,*], Hui-Xing Zhu [a,b], Yue Su [c], Yi-Long Yuan [a,b], Tian-Fu Xu [a,b,**]

[a] Key Laboratory of Groundwater Resources and Environment, Ministry of Education, Jilin University, Changchun, 130021, Jilin, China
[b] Jilin Provincial Key Laboratory of Water Resources and Environment, Jilin University, Changchun, 130021, Jilin, China
[c] Changzheng Engineering Technology CO., LTD.LANZHOU, Lanzhou, 730030, Gansu, China

ARTICLE INFO

Article history:
Received 6 March 2025
Received in revised form
3 June 2025
Accepted 3 September 2025
Available online 10 September 2025

Edited by Jie Hao and Xi Zhang

Keywords:
Natural gas hydrates
Permeability
Multi-phase flow
Multi-scale

ABSTRACT

Natural gas hydrate production involves complex mass/heat transfer, phase transformation, and multiphase seepage processes, where permeability critically influences exploitation efficiency and sediment stability. This review summarizes progress in permeability evolution in hydrate-bearing sediments, covering: multiphase seepage theories involving absolute and relative permeability models; pore-scale methods, including Lattice Boltzmann, Pore Network models, CFD simulations, and microfluidic experiments, for investigating the effects of hydrate morphology and pore heterogeneity; core-scale experiments, such as seepage tests and X-ray CT, for quantifying permeability changes with hydrate saturation and stress sensitivity; site-scale scenarios involving pilot tests and numerical models are challenged by fluid migration prediction and reservoir stability. Key findings show hydrate dissociation induces dynamic pore structure changes and complex multiphase interactions, with existing models oversimplifying heterogeneous pore structures and hydrate distributions. Critical research gaps include: inadequate characterization of pore structure evolution during hydrate nucleation/dissociation; unclear gas-water flow mechanisms in deformable sediments; lack of multiscale correlation and coupled modeling for permeability-stress-phase change interactions. Addressing these offers critical insights for optimizing extraction, reducing energy use, and ensuring reservoir stability, enabling safe and efficient exploitation of natural gas hydrates as a strategic clean energy resource.

1. Introduction

Natural gas hydrate (NGH) represents a caged crystalline compound which is engendered by light hydrocarbon gases (predominantly methane) and water molecules under the conditions of low temperature (<27 °C) and high pressure (>0.6 MPa) (Parisa et al., 2024; Ge et al., 2024; Jiao et al., 2025). Owing to its attributes of high energy density, wide distribution range and substantial resource potential, hydrate has been deemed an exceedingly crucial new genre of clean energy unearthed in recent decades (Gao, 2022; Krishna et al., 2024; Zhang et al., 2024a). Moreover, it is capable of functioning as a transitional energy within the energy system throughout the transition from extant fossil energy to commercially renewable energy (Dong et al., 2024; Jiang et al., 2024; Lei et al., 2024; Li et al., 2025).

The production process of natural gas hydrate is complex, entailing mass and heat transfer, phase transformation as well as multi-phase seepage (Fig. 1). Regarding mass and heat transfer, the hydrate production requires energy input to change the environment. For instance, during thermal stimulation exploitation, heat transfer facilitates the hydrate decomposition, the generated methane gas and water flow in the pores (Li et al., 2022b; Wu et al., 2022a; Moridis et al., 2023). In this process, mass transfer and heat transfer reciprocally influence each other. The endothermic decomposition of hydrate alters the temperature distribution and subsequently impacts the further progression of heat transfer (Cai et al., 2024; Li et al., 2024d; Sun et al., 2024a). Regarding phase transformation, the production causes solid hydrate to decompose into methane gas and water. This process is subject to multiple factors and exhibits dynamic alterations (Ohtsuki et al., 2024; Zhang et al., 2024c; Sun et al., 2025). There also exist scenarios

* Corresponding author.
** Corresponding author.
E-mail addresses: xxxx@jlu.edu.cn (X. Xin), tianfu_xu@jlu.edu.cn (T.-F. Xu).
Peer review under the responsibility of China University of Petroleum (Beijing).

https://doi.org/10.1016/j.petsci.2025.09.007

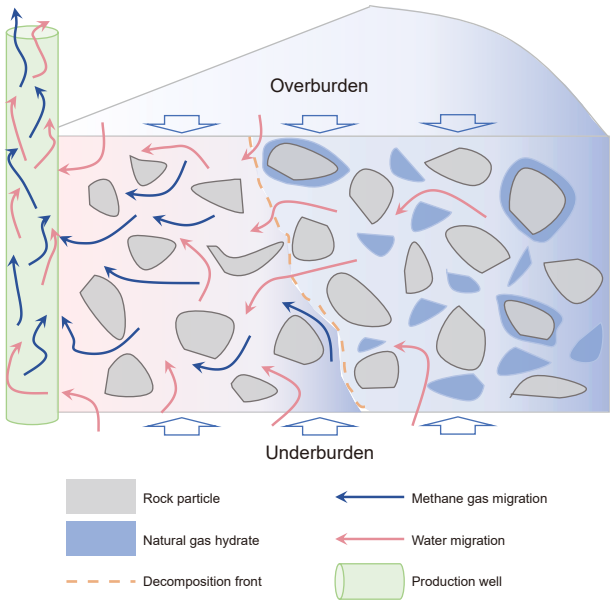

Fig. 1. Multi-component and multi-phase systems in hydrate-bearing sediments. The interactions among rock particles, hydrate, gas, and water during hydrate production.

of three-phase coexistence, wherein a minute alteration in temperature and pressure would disrupt the equilibrium (Lu et al., 2023; Xia et al., 2023; Moridis et al., 2024); Regarding multi-phase seepage, the hydrate decomposition modifies the permeability. There exist interactions, such as capillary forces, among multi-phase fluids, and difference in viscosity results in different velocity and pressure distributions, which interact with mass and heat transfer as well as phase transformation (Li et al., 2023c, 2024b; Gorenkov et al., 2024). These three facets are intimately intertwined and collectively constitute the intricate production process.

Permeability, as a physical index, gauges the capacity of a porous medium to permit the fluids flow. During the hydrate production process, it directly affects the flow of gas and water fluids within the hydrate bearing sediments. After the hydrate decomposition, methane gas and water would be generated, and these fluids flow through the pore channels of the sediments to the production wells. The magnitude of permeability dictates the facility of fluid flow, and the production efficiency is intimately correlated with the flow rate of fluids. A higher permeability is conducive to the rapid discharge of methane gas and water, thus enhancing the production efficiency. Conversely, in the event that the permeability is lower, the flow of gas and water is blocked, the discharge speed will slow down, and more time and energy will be required to extract the same amount of methane gas. During the production process, the hydrate decomposition modifies the permeability. A sudden change (such as a significant increase) in permeability may lead to a change in the pore pressure and trigger formation instability. Accurate comprehension of the permeability evolution characteristics is of paramount significance for optimizing the hydrate production process, reducing energy consumption and maintaining the sediments stability (Gambelli, 2023; Meng et al., 2024; Sakurai et al., 2024).

The alterations in multiple factors, including temperature, pressure, pore structure, and fluids components give rise to complex physical and chemical phenomena during hydrate dissociation. Studying at different scales is essential, with each scale providing unique insights and advantages. At the pore scale, the research focuses on the hydrate crystal morphology, variations in pore structure, and the microscopic seepage mechanism. It is capable of precisely revealing the microscopic action mechanism during hydrate formation and decomposition, thereby facilitating the establishment of accurate microscopic physical models and providing a crucial foundation for comprehending basic physical processes (Cai et al., 2024). At the core scale, the research lays emphasis on the determination of parameters like hydrate saturation and core permeability. On a relatively large and controllable scale, it comprehensively takes into account the interactions among hydrate, fluid, and rock, and also provides direct data support for validating theoretical models and conducting numerical simulations (Wang et al., 2023; Gu et al., 2025). At the site scale, the research primarily focuses on the distribution of hydrate reservoirs, formation stability, and the environmental impacts of large-scale exploitation. From a practical application perspective, it furnishes comprehensive and systematic decision-making bases for the commercial production, geological disaster prevention, and energy strategic layout (Liu et al., 2017, 2022, and 2023). In recent years, both domestic and international researchers have probed into the characteristics of hydrate phase transition and multi-phase seepage across diverse scales with regard to the scientific issue of “Permeability evolution in hydrate bearing sediments”, thereby yielding abundant results.

To sum up, this review endeavors to sort out the latest research progress in the field of “permeability evolution in hydrate bearing sediments”, encompassing the absolute and relative permeability evolution within the framework of multi-phase seepage theory; pore-scale simulations, including the Lattice Boltzmann Model (LBM), Pore Network Model (PNM), Computational Fluid Dynamics simulation (CFD), and microfluidic chip experiments; combined seepage calculations integrating core seepage experiments and pore structure imaging at the core scale; hydrate production tests and numerical simulations of production processes at the site scale. These aspects comprehensively present the current state and development trends of research in this field to readers (Fig. 2).

2. Multi-phase seepage theory

Regardless of the production method employed for natural gas hydrate, issues pertaining to phase transition and gas-water multi-phase seepage are invariably entailed. During the process wherein solid hydrate decomposes into methane gas and liquid water, the pore structure and multi-phase seepage parameters undergo dynamic evolution. The evolution of pore structure induced by hydrate decomposition exerts a direct impact on absolute permeability and relative permeability. The alteration in permeability is influenced by capillary pressure, and the relative permeability of the gas and water phases display intricate variation patterns.

2.1. Absolute permeability evolution

Absolute permeability serves as a pivotal indicator for mirroring the capacity of a porous medium to permit the fluids flow. In accordance with the occurrence state of hydrate within the sediments, absolute permeability k can be categorized into effective permeability $k(S_h)$ when hydrate is present and intrinsic permeability k_0 when hydrate is absent (Li et al., 2023c).

The permeability of hydrate-bearing sediments, which may differ in terms of lithology, locations within the same lithology, even burial depths within the same lithology and location, exhibits variability. It is futile to directly compare their values. Consequently, normalized permeability k_{nor} is introduced to depict the

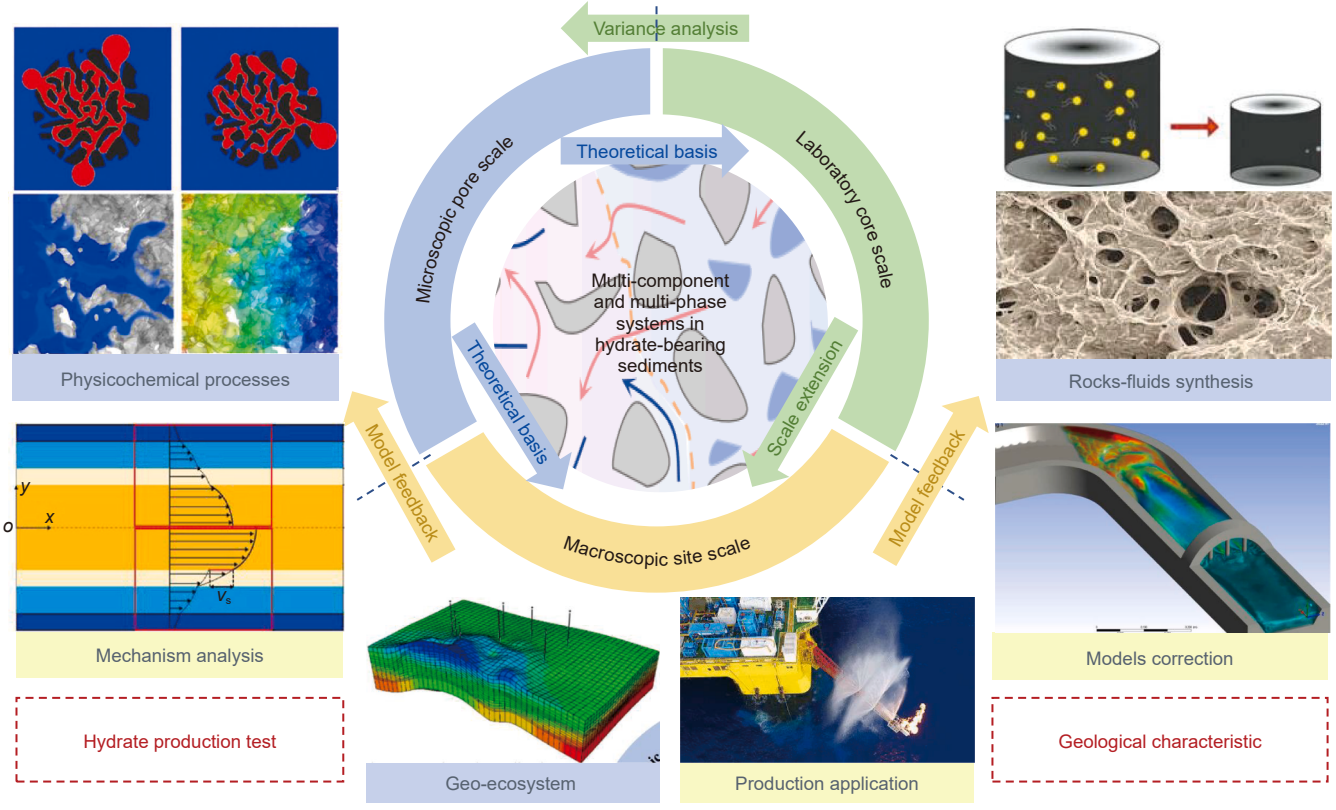

Fig. 2. Multi-scale studies of hydrate-bearing sediments. Integrating pore-scale mechanisms, core-scale experiments, and site-scale applications with model feedback.

dynamic evolution characteristics of absolute permeability during the hydrate decomposition process (Lu et al., 2019):

$$k_{nor} = \frac{k(S_h)}{k_0} \tag{1}$$

The principal models employed for characterizing the absolute permeability evolution encompass the parallel capillary tube model and the Kozeny particle model (Gong et al., 2023; Li et al., 2024c).

2.1.1. Parallel capillary tube model

This model characterizes the pore space in terms of n parallel capillary tubes, each of which has an inner diameter of r and a length of L. On the basis of this portrayal, the fluid flow rate q can be computed:

$$q = \frac{n\pi r^4 \Delta P}{8\mu L} \tag{2}$$

where $\frac{\Delta P}{L}$ is the pressure gradient, Pa/m.

At this flow rate, the absolute permeability of sediments with porosity ϕ is:

$$k = \frac{\phi r^4}{8} \tag{3}$$

Kleinberg et al. (2003) further deduced the permeability evolution when hydrates grow uniformly at the wall of the sediments and in the center of the capillary tube:

$$k(S_h) = k_0(1 - S_h)^2 \tag{4}$$

$$k(S_h) = k_0\left[1 - {S_h}^2 + \frac{2(1 - S_h)^2}{\lg S_h}\right] \tag{5}$$

Masuda optimized Eq. (4) and put forward a mathematical model indicating that there is an exponential relationship between the permeability and the hydrate saturation, namely the Masuda model (Masuda, 1997):

$$k_{nor} = (1 - S_h)^N \tag{6}$$

where N is the attenuation index, its value varies in different types of hydrate-bearing sediments.

2.1.2. Kozeny particle model

In actual hydrate-bearing sediments, the pore space predominantly assumes an irregular shape, and there are scarcely any channels analogous to parallel capillaries. The actual distance over which the fluid flows within the pores of the sediments is significantly greater than the direct two-point connection distance utilized for calculating the pressure gradient. Consequently, it becomes more intricate to elucidate the permeability evolution when taking into account the shape of sediment particles.

Kleinberg et al. (2003) took the Kozeny–Carman Eq. (7) as a foundation, conceived of the entire seepage field as a single capillary, and deduced three forms, which were represented by the ratio of pore surface area A_{pore} to pore volume V_{pore}, sediments volume V_{all}, and particle volume V_{rock} in the Kozeny particle model Eqs. (8–10):

$$k = \frac{\phi V_{\text{pore}}^2}{\gamma \tau A^2} \tag{7}$$

where V_{pore} is the pore volume; γ is the form factor; τ is the bending degree; A is the pore surface area.

$$k = \frac{\phi}{\gamma \tau \left(\frac{A_{\text{pore}}}{V_{\text{pore}}}\right)^2} \tag{8}$$

$$k = \frac{\phi^3}{\gamma \tau \left(\frac{A_{\text{pore}}}{V_{\text{all}}}\right)^2} \tag{9}$$

$$k = \frac{\phi^3}{\gamma \tau (1-\phi)^2 \left(\frac{A_{\text{pore}}}{V_{\text{rock}}}\right)^2} \tag{10}$$

Dai and Seol (2014) undertook a substantial amount of numerical simulation work to modify the Kozeny–Carman equation, and subsequently proposed a normalized permeability evolution model:

$$k_{\text{nor}} = \frac{(1-S_{\text{h}})^3}{(1+2S_{\text{h}})^2} \tag{11}$$

This research takes into consideration the heterogeneous characteristics of the pore structure and the occurrence pattern of hydrates within hydrate bearing sediments, does not impose limitations on the hydrate formation pattern and comprehensively contemplates the alterations in pore space and bending degree. This model does not involve empirical parameters and exhibits strong practical applicability.

2.1.3. Other evolution models

In addition to the two aforementioned common evolution models, there exist several other models that are capable of more effectively representing the effective permeability evolution characteristics permeability during the hydrate decomposition (Cai et al., 2020b). For instance, the Van Genuchten (VG) model, which is adopted by the Lawrence Berkeley Laboratory within the Tough2 code (Van, 1980):

$$k_{\text{nor}} = \sqrt{S_{\text{nw}}}\left[1-\left(1-\sqrt[m]{S_{\text{nw}}}\right)^m\right]^2 \tag{12}$$

$$S_{\text{nw}} = \frac{S_{\text{w}} - S_{\text{wr}}}{1 - S_{\text{wr}}} \tag{13}$$

where S_{w} is the liquid phase saturation; S_{nw} is the normalised water-phase saturation; S_{wr} is the irreducible water saturation; m is an empirical coefficient and is usually assigned a value of 0.46 in common sandstone, siltstone and conglomerate sediments (Liu, 2024).

Delli and Grozic (2013) took into consideration the occurrence patterns of hydrates in both pore-filling and grain-coating forms, and derived a comprehensive normalized permeability evolution model based on the weights of these two patterns:

$$k_{\text{nor}} = {S_{\text{h}}}^n k_r^{\text{pf}} + (1-S_{\text{h}})^m k_r^{\text{gc}} \tag{14}$$

where k_r^{pf} and k_r^{gc} are the normalized permeability under two hydrate occurrence modes respectively; ${S_{\text{h}}}^n$ and $(1-S_{\text{h}})^m$ are the weight coefficients corresponding to the two hydrate occurrence patterns respectively. The specific values of m and n can be adjusted according to the characteristics of the actual site.

Katagiri et al. (2017) focused on cubic packs of cylinders and spheres, and developed permeability reduction models for grain-coating and pore-filling hydrates:

$$k_{\text{nor}} = \frac{\pi(1-S_{\text{h}})^{n+2}}{4-(4-\pi)(1-S_{\text{h}})} \tag{15}$$

$$k_{\text{nor}} = \frac{(1-S_{\text{h}})^{n+2}}{\left[1+\sqrt{\frac{(4-\pi)S_{\text{h}}}{\pi}}\right]^2} \tag{16}$$

The expression, advantages and disadvantages of commonly used effective permeability evolution models were summarized in Table 1.

2.2. Relative permeability evolution

Fig. 3 depicts the gas and liquid phase fluid flow in hydrate-bearing sediments. Utilizing Darcy's law to compute the multi-phase flow, it is necessary to take the phase saturation into account when calculating the area traversed by each phase of fluid. The multi-phase fluid flow does not represent a simple superposition of the flow of each individual single-phase fluid. Interactions exist among the fluids of each phase, which impede the flow of one another. Consequently, it is infeasible to accurately describe the multi-phase fluid flow merely by multiplying the phase saturation on the basis of single-phase flow.

With the aim of characterizing the retardation effect among different phases fluids during the multi-phase fluid flow, it becomes essential to modify the Darcy velocity by multiplying a coefficient:

$$v = -k_{r\beta}\frac{k}{\mu_\beta}\cdot(\nabla P - \rho g\cos\theta) \tag{17}$$

where $k_{r\beta}$ is the relative permeability of β phase fluids.

Given that solid hydrate and rock particles are present within the sediments, gas-liquid-solid three-phase interfaces are bound to exist in the gas-liquid phase fluid flow process. In this region, capillary pressure is generated, which will exert an impact on the pressure gradient during the flow process. Consequently, it is imperative to modify the aforementioned formula so as to derive the multi-phase Darcy's law that characterizes the multi-phase fluid flow process:

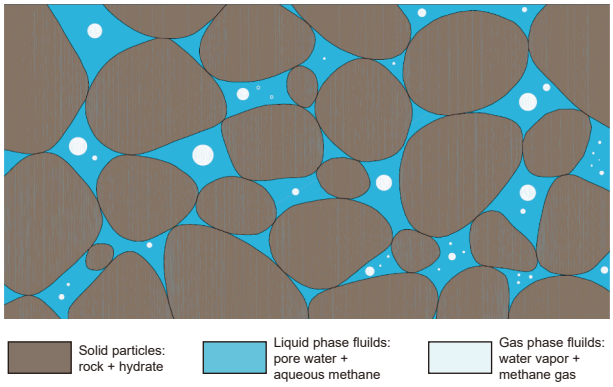

Fig. 3. Gas-liquid phase fluid flow in hydrate-bearing sediments. Distributions solid particles (rock + hydrate), liquid phase (pore water + aqueous methane), and gas phase (water vapor + methane gas).

$$v = -k_{r\beta}\frac{k}{\mu_\beta}\cdot\left[\nabla\left(P + P_{c\beta}\right) - \rho g\cos\theta\right] \tag{18}$$

where $P_{c\beta}$ is the capillary pressure of β phase fluids.

The principal models employed for characterizing the relative permeability evolution encompass the Corey model, the optimized Van Genuchten model, and the modified Stone model (Xia, 2022).

2.2.1. Corey model

Corey depicted the relative permeability evolution according to the empirical model of unsaturated sediments (Corey, 1986):

$$k_{rw} = \bar{S}^4 \tag{19}$$

$$k_{rg} = (1-\bar{S})^2\left(1-\bar{S}^2\right) \tag{20}$$

$$\bar{S} = \frac{S_w - S_{rw}}{1 - S_{rw} - S_{rg}} \tag{21}$$

2.2.2. Optimized Van Genuchten model

Based on the Van Genuchten model, Moridis et al. put forward the OPM and EPM models for calculating the relative permeability (Moridis, 1998):

$$k_{rw} = \bar{S}^{1/2}\left[1-\left(1-\bar{S}^{1/m}\right)^m\right]^2 \tag{22}$$

$$k_{rg} = (1-\bar{S})^{1/2}\left(1-\bar{S}^{1/m}\right)^{2m} \tag{23}$$

$$\bar{S} = \frac{S_w - S_{rw}}{1 - S_{rw}} \tag{24}$$

2.2.3. Modified stone model

Gamwo and Liu (2010), Mahabadi and Jang (2014) introduced the modified Stone model to calculate the evolution of gas and water relative permeability in hydrate-bearing sediments:

$$k_{rw} = \left(\frac{S_w - S_{rw}}{1 - S_{rw} - S_{rg}}\right)^{n_w} \tag{25}$$

$$k_{rg} = \left(\frac{S_g - S_{rg}}{1 - S_{rw} - S_{rg}}\right)^{n_g} \tag{26}$$

where k_{rw} and k_{rg} are the relative permeability of water and gas phase respectively; S_w and S_g are the saturation of water and gas phase respectively; S_{rw} and S_{rg} are the irreducible saturation of water and gas phase respectively; n_w and n_g are the attenuation index of water and gas phase relative permeability respectively.

In the commonly adopted models regarding the relative permeability evolution of gas and water phase in relation to water phase saturation, the values of model parameters exert a significant influence. Consequently, in light of diverse actual site information, it is imperative to conduct fittings on the multi-phase seepage test data obtained from the site for the calibration of model parameters. Only the calibrated model can then be appropriately applied to the simulation of the hydrate production.

2.2.4. Other evolution models

In addition to the three aforementioned common evolution models, there exist several other models that are capable of more effectively representing the relative permeability evolution characteristics during the hydrate decomposition. Singh et al. developed an analytical model concerning the gas and water phase relative permeability evolution through the combination of the steady-state form of the Navier–Stokes equation and the momentum conservation equation. The relative permeability evolution of sediments containing grain-coating hydrates is presented as follows (Singh et al., 2019):

$$k_{rg} = \frac{r_g^2}{R^2}\left[\alpha\left(1-\frac{r_w^2}{r_g^2}\right)-1\right]\frac{\tau(\phi, 1-S_h-S_{wr})}{\tau(\phi, S_g)} \tag{27}$$

$$k_{rw} = \frac{\left(r_w^2 - r_g^2\right)^2}{R^2\left(r_w^2 - r_g^2\right)}\frac{\tau(\phi, 1-S_h-S_{wr})}{\tau(\phi, S_w)} \tag{28}$$

The expression, advantages and disadvantages of commonly used relative permeability evolution models were summarized in Table 2.

This section presents multi-phase seepage theories, focusing on absolute and relative permeability models critical for understanding permeability evolution in hydrate-bearing sediments. Absolute permeability models (parallel capillary tube, Kozeny particle, Van Genuchten) emphasize hydrate occurrence patterns (grain-coating/pore-filling) influencing pore structure and fluid flow capacity; normalized permeability frameworks capture dynamic changes during hydrate dissociation. For relative permeability, the Corey model, optimized Van Genuchten model, and modified Stone model characterize gas-water flow interactions, though often oversimplifying heterogeneous pore structures and lacking hydrate saturation-seepage parameter feedback. These frameworks provide foundational insights but require integration with micro-scale mechanisms and field data to improve accuracy in complex reservoirs.

3. Microscopic pore scale

The research at the pore scale primarily centers around microscopic physicochemical processes, exemplified by the hydrogen bonding between hydrate molecules and the surrounding water molecules. This type of interaction exerts an impact on the stability and decomposition characteristics of hydrate bearing sediments. When investigating the microscopic seepage mechanism, it entails the flow behavior of fluid molecules within narrow pore channels, which is subject to the influence of intermolecular interactions (such as van der Waals forces) and surface tension. Research conducted at this scale pertains to the most microscopic structures and processes, with a focus on molecular and atomic levels as well as pore characteristics spanning from nanometers to micrometers.

At the microscopic pore scale, fluids are typically discretized into a series of mass particles, and statistical calculation methodologies are employed to compute the flow. In recent years, computational methods including the Lattice Boltzmann Method (LBM), Pore Network Model (PNM), and Computational Fluid Dynamics simulations (CFD) have been prevalently utilized to assess the impact of diverse factors on the permeability characteristics during the hydrates decomposition within porous media. Moreover, microfluidic chip experiments are capable of precisely controlling conditions such as fluid flow, temperature, and pressure at a minuscule scale, simulating the hydrates formation and decomposition processes within microscopic pores, and monitoring parameter changes in real time.

3.1. Lattice Boltzmann method (LBM)

Yang et al. (2021, 2022, 2024a) predicated on the classical nucleation theory capable of computing the probability of hydrate formation positions within the gas-water-sand three-phase system and the phase-field model furnishing the migration rate of the hydrate formation front, integrated processes encompassing multi-phase and multi-component seepage, heat and mass transfer, heterogeneous reactions, and solid-phase structure evolution. They analyzed the impacts of solute transport, water saturation, and heat transfer factors, among others, on the hydrate decomposition and devised the LBM model applicable for computing the formation and decomposition processes of hydrates within sediments.

Ji et al. (2021, 2022) and Yuan et al. (2022) centered their attention on the hydrate phase transformation and pore structure evolution. Employing the LBM model, they simulated the hydrate decomposition under depressurization, ascertained the impacts of diverse pore structure shapes, hydrate forms and occurrence states on the relative permeability, and arrived at the conclusion that the arrangement of mineral particles exerts no significant influence on the permeability change. Xin et al. (2021b) and Li et al. (2024b) predicated on the size and tortuosity of the control seepage channel, they put forward the evolution models of absolute and relative permeability under the two hydrate distribution patterns of grain-coating and pore-filling.

Li et al. (2023a, 2024h, 2024i) utilized the LBM model integrating fluid dynamics and thermodynamics to simulate the hydrates decomposition process under the conditions of hot fluid injection, depressurization, and the combined exploitation. They analyzed the pore structure evolution characteristics of three prevalent hydrate distribution patterns (pore-filling, grain-coating, and dispersed type, Fig. 4(a)–(d)), and ascertained that the coupling of mass and heat transfer exerts a significant influence on the pore structure evolution, as manifested in the pore connectivity.

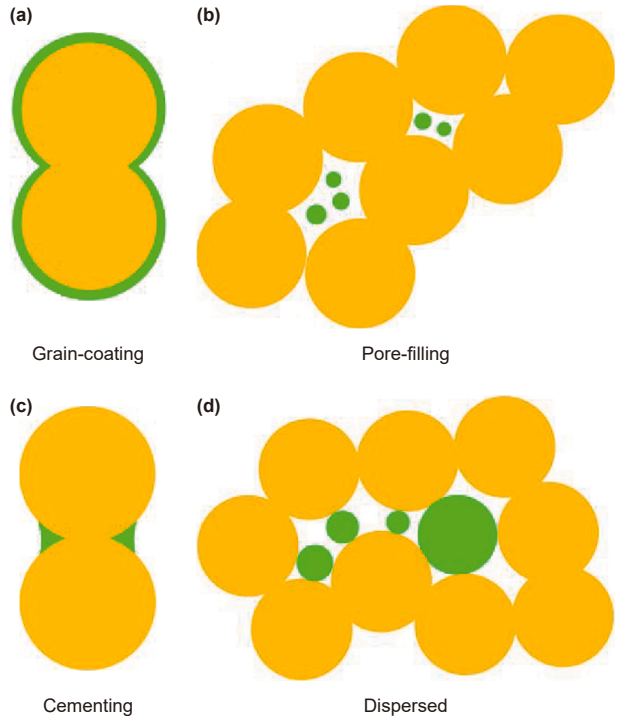

Fig. 4. Natural gas hydrate distribution patterns in hydrate-bearing Sediments. **(a)** Grain-coating, **(b)** pore-filling, **(c)** cementing and **(d)** dispersed type (Ren et al., 2020).

These studies, with the recourse to the LBM model, expounded in detail the correlation between the pore structure and seepage characteristics during the hydrate phase transition process from diverse perspectives, namely the pore structure characteristics, the construction of permeability evolution models, and the analysis of influencing factors, thereby furnishing a reference basis for accurately portraying the heat and mass transfer of hydrate bearing sediments at the macroscopic scale.

3.2. Pore network model (PNM)

Abdoli et al. (2018) and Liu et al. (2024) utilized the PNM to delineate the microscopic pore structures of hydrate bearing sediments, simulated the hydrates decomposition of diverse occurrence patterns, examined the anisotropy of absolute permeability, capillary pressure, and relative permeability during the hydrate decomposition, and computed the impacts of pore size distribution, depressurization amplitude, and initial hydrate saturation on the gas-water production and gas saturation during hydrate decomposition.

Luo et al. (2022), Zhang et al. (2022c), and Tian et al. (2023) employed the stochastic simulation method to fabricate digital cores of grain-coating and pore-filling hydrates. By recourse to the PNM, they retrieved the pore radius, throat radius, and the number of pore connections, investigated the pore space evolution process, scrutinized the influences of model dimension, number of nucleation, and hydrate occurrence patterns on the effective permeability, and ultimately established the normalized permeability and resistivity index models for different hydrate occurrence patterns respectively.

These studies, with the recourse to the PNM model, furnished theoretical basis and data support for a profound understanding of the hydrate-bearing sediments characteristics and production prediction from diverse perspectives, namely the characterization of microscopic pore structures, hydrate formation, and anisotropy analysis.

3.3. Computational fluid dynamics simulation (CFD)

Zhang et al. (2022a), Xu et al. (2023a), and Liu et al. (2024a) employed the CFD method to formulate two-dimensional geometric models depicting hydrate occurrence patterns and heterogeneous hydrate bearing sediments models with varying particle size distributions. They examined the dynamic evolution of pore structures and seepage characteristics, and ascertained that the reduction in permeability is predominantly determined by the hydrate distribution patterns, and a log-linear relationship exists between sediment particle size and effective permeability. For the quantitative analysis of the pore structure, an improved effective permeability evolution model was deduced by integrating the specific surface area with the particle size distribution characteristics.

By integrating Computational Fluid Dynamics with the Discrete Element Method (CFD-DEM), Chen et al. (2024), Liu et al. (2024b) and Song et al. (2024b) investigated the migration and production laws of fine sand in the vicinity of the well-bore during the methane hydrate production process, thereby revealing the movement process and microscopic mechanism of sand grains within gas-liquid two-phase flow. Wang et al. (2024c) and Guo et al. (2025) elucidated that fine grain migration has dual effects: enhancing permeability or causing sand arch collapse and erosive eruptions.

These studies, with the recourse to CFD models, have enhanced the understanding of the seepage characteristics and the sand grain migration mechanism of hydrate bearing sediments. The CFD method is frequently utilized to integrate with the DEM method for resolving the sand production process and mechanical responses, given that it can comprehensively and accurately manage multi-phase flow and particle motion, strike a balance between computational efficiency and resource requirements, and possess strong adaptability and flexibility.

3.4. Microfluidic chip experiments

Microfluidic chip experiments integrate microfluidic and chip technologies, thereby enabling precise manipulation and analysis of fluids on miniaturized chips.

Xu et al. (2023b), Yang et al. (2024b), and Zhang et al. (2024d, 2024e) developed high-pressure microfluidic experimental systems. Through observation, they identified different formation mechanisms of methane hydrates within pores and ascertained that the hydrates formation demands a phase equilibrium state and disturbances, with the disturbance effect of constant pressure flow being stronger. Moreover, they visually investigated the decomposition behavior of cyclopentane hydrates and noted that stable emulsions are formed during hydrate dissociation, as well as that salts and surfactants possess different influence mechanisms regarding the hydrate dissociation.

Microfluidic chip experiments enable detailed investigations of pore-scale hydrate-bearing sediment interactions in three key domains: First, they enable controlled visualization of hydrate nucleation and morphological transitions, differentiating between grain-coating and pore-filling growth patterns to calibrate theoretical models. Second, quantitative analysis of multiphase flow during hydrate dissociation employs high-speed imaging to monitor gas-liquid interface dynamics, uncover preferential flow pathways and transient permeability variations, and quantify capillary hysteresis for refining dynamic flow models. Third, particle-scale stress-strain experiments under controlled conditions establish correlations between hydrate morphology and sediment mechanics by directly observing the mechanical responses of microstructures.

At the microscopic pore scale, computational methods (LBM, PNM, CFD) and microfluidic experiments analyze hydrate morphology effects on pore-scale seepage mechanisms. LBM simulations show grain-coating and pore-filling hydrates differentially impact pore connectivity and relative permeability, with coupled mass-heat transfer influencing decomposition-induced pore structure evolution. PNM and CFD quantify permeability anisotropy and size effects in heterogeneous pores; microfluidic chips enable controlled observation of hydrate nucleation/dissociation, identifying stable emulsions and capillary hysteresis during phase transitions. These methods bridge molecular- and core-scale behaviors but face challenges in modeling real sediment complexity and transient hydrate-fluid interfaces, underscoring the need for integrated pore-scale data in upscaling.

4. Laboratory core scale

The research at the core scale regard hydrates as an integrated entity that interacts with rocks and fluids, while taking into account the hydrates distribution within the relatively intact geological unit of the core. Through the employment of diverse analytical and testing techniques on core samples, crucial information concerning the physical properties, chemical compositions, and pore structures of the rocks can be obtained. The scope of such studies has been expanded from microscopic pores to the entirety of the core containing multiple pores, with the research focus shifting from microscopic interactions among molecules and atoms to the macroscopic interaction between hydrates, rocks, and fluids.

4.1. Core seepage experiments

Based on the drilling and production data from a variety of hydrate sites, such as the Ottawa 20/30 station (Geranutti et al., 2024), the KG Basin NGHP-02 station (Li et al., 2019; Yoneda et al., 2019), and the Shenhu Sea SH2 station (Deng et al., 2024; Ren et al., 2024), sandy cores with diverse porosity and hydrate saturations were artificially fabricated. Comprehensive investigations into the evolution characteristics of temperature and pressure during the hydrate dissociation process through heat injection or depressurization were carried out. The absolute and effective permeability of the samples under different hydrate saturation were calculated and curve fitting between the experimental results and theoretical models was executed.

Focusing on typical sandy hydrate sites such as the Nankai Trough, fine-grained quartz sand was employed to synthesize cores, and hydrates were produced using either tetrahydrofuran (THF) or methane gas (Kou et al., 2024; Song et al., 2024a; Wang et al., 2024d). The hydrate saturation and pore capillary pressure were computed during the synthesis process, and it was noted that hydrate formation resulted in a reduction of the core's effective pore space, which was concurrent with an increase in capillary pressure. Additionally, the differential evolution of the hydrate morphology and relative permeability was analyzed, and the fitting parameters for the Van Genuchten model under different hydrate saturations were put forward. Nevertheless, due to the stochastic nature of hydrate formation, a quantitative relationship between capillary pressure/relative permeability and hydrate saturation has not yet been established in these multi-phase seepage studies.

Using the excess gas method, sandy and silt cores with varying hydrate distribution patterns and saturation were synthesized (You et al., 2023; Peng et al., 2024), measurements showed effective permeability declined rapidly with increasing hydrate saturation (Lei et al., 2021; Li et al., 2021; Zhao et al., 2024b). A triaxial permeability apparatus was used to investigate effects of effective confining pressure and triaxial compression on core permeability, confirming gas permeability decreased as effective stress increased (Wu et al., 2022b; Li et al., 2024g; Wang et al., 2024b). These studies quantified the permeability of cores under diverse hydrate saturation and elucidated the evolutionary relationship between effective permeability and hydrate saturation. Nevertheless, the understanding of the evolutionary relationship between the relative permeability of the gas and water phases and hydrate saturation remains nebulous (Zhao et al., 2024a).

4.2. Pore structure imaging combined with seepage calculation

Depressurization decomposition was carried out on clayey silt and sandy hydrate-bearing cores, and X-ray CT scanning technology was utilized to obtain images of pore structure evolution during the hydrate phase transition process (Cai et al., 2020a; Lei et al., 2022a; Hu et al., 2024). Methods including the LBM, PNM, and CFD were adopted to measure permeability under different gas pressures and saturations (Aghajanloo et al., 2024; Liu et al., 2024; Wang et al., 2024a). Additionally, the distribution characteristics of gas and water phase fluids were analyzed (Zhang et al., 2023; Li et al., 2024f; Wu et al., 2024b). It was determined that changes in the shape and size of dominant seepage channels were the primary factors contributing to differential permeability

Table 1
Summary of effective permeability evolution models.

Model	Expression	Advantages	Disadvantages
Kleinberg et al. (2003)	Grain-coating: $k_{nor} = \frac{k(S_h)}{k_0} = (1-S_h)^2$ Pore-filling: $k_{nor} = 1 - {S_h}^2 + \frac{2(1-S_h)^2}{\lg(S_h)}$	Considering pore structure and hydrates patterns	Detachment from reality
Masuda (1997)	$k_{nor} = (1-S_h)^N$	Distinguishing hydrate morphology	Logarithmic term cause numerical instability
Katagiri et al. (2017)	Grain-coating: $k_{nor} = \frac{\pi(1-S_h)^{n+2}}{4-(4-\pi)(1-S_h)}$	Simple form; flexible via parameter N	Ignoring pore structure and hydrates patterns; unclear physical meaning
Van (1980)	Pore-filling: $k_{nor} = \frac{(1-S_h)^{n+2}}{\left[1+\sqrt{\frac{(4-\pi)S_h}{\pi}}\right]^2}$		
Delli and Grozic (2013)	$k_{nor} = \sqrt{S_{nw}}\left[1-\left(1-\sqrt[m]{S_{nw}}\right)^m\right]^2$ $k_{nor} = {S_h}^n k_r^{pf} + (1-S_h)^m k_r^{gc}$	Considering pore structure and hydrates patterns Capturing non-linear relationships	Complex formulas; difficult parameter calibration Complex computation
Dai and Seol (2014)	$k_{nor} = \frac{(1-S_h)^3}{(1+2S_h)^2}$	Considering mixed hydrate patterns	Complex form

evolution (Zhao et al., 2023; Li et al., 2024e; Xia et al., 2024). Furthermore, the stress sensitivity characteristics of relative permeability and the anisotropic variation law of permeability were ascertained (Zhang et al., 2024f).

5. Macroscopic site scale

The research at the site scale principally center on the practical application issues pertaining to hydrate reservoirs during actual exploitation and geological activities. From the vantage point of the entire hydrate reservoir along with its geological and ecological environments, the impacts of activities like hydrate exploitation on extensive areas are considered. It perceives the hydrate reservoir as an integral part of a complex geological-ecological system, and the research scope encompasses the distribution laws of hydrate reservoirs within expansive geological regions, the influence of the production process on the sediments stability, and the comprehensive repercussions on the surrounding environment.

The principal research methodologies at the site scale encompass site production tests and numerical simulation.

5.1. Hydrate production tests

Hydrate production tests pertains to the conduction of exploitation at the actual hydrate reservoir. Its advantage resides in its capacity to directly procure production data regarding of hydrate reservoirs within the actual geological environment, exemplified by production rates, methane gas productivity, and settlement magnitudes. The data acquired is authentic and reliable, being capable of visually manifesting exploitation phenomena, and facilitating the accumulation of practical experience for large-scale production. Nevertheless, production tests entails high economic costs and may potentially induce irreversible impacts on the surrounding environment.

A cumulative total of 10 hydrate production tests have been accomplished on a global scale (Wu et al., 2020). Of these, 4 were implemented in deep sea and 6 in permafrost areas on land (Li et al., 2022a; Tamaki et al., 2022). The land production sites encompass the Mallik Delta in Canada (conducted in 2002, 2007, and 2008), the northern slope of Alaska in the United States (conducted in 2007), and the Muli Basin in the Qilian Mountains of China (conducted in 2011 and 2016). The offshore production sites encompass the Nankai Trough in Japan (carried out in 2013 and 2017) and the Shenhu Sea area in the South China Sea of China

Table 2
Summary of relative permeability evolution models.

Model	Expression	Advantages	Disadvantages
Corey model	Gas phase: $k_{rg} = \left[1-\left(\frac{S_w-S_{rw}}{1-S_{rw}-S_{rg}}\right)\right]^2\left[1-\left(\frac{S_w-S_{rw}}{1-S_{rw}-S_{rg}}\right)^2\right]$ Liquid phase: $k_{rw} = \left(\frac{S_w-S_{rw}}{1-S_{rw}-S_{rg}}\right)^4$	Simple mathematical form	Overly simplistic; fail to capture complex, non-linear behaviors
Optimized Van Genuchten model	Gas phase: $k_{rg} = \left(1-\frac{S_w-S_{rw}}{1-S_{rw}}\right)^{1/2}\left(1-\frac{S_w-S_{rw}}{1-S_{rw}}^{1/m}\right)^{2m}$ Liquid phase: $k_{rw} = \frac{S_w-S_{rw}}{1-S_{rw}}^{1/2}\left[1-\left(1-\frac{S_w-S_{rw}}{1-S_{rw}}^{1/m}\right)^m\right]^2$	Flexibility to fit diverse data by adjusting exponents	Calibration complexity
Modified Stone model	Gas phase: $k_{rg} = \left(\frac{S_g-S_{rg}}{1-S_{rw}-S_{rg}}\right)^{n_g}$ Liquid phase: $k_{rw} = \left(\frac{S_w-S_{rw}}{1-S_{rw}-S_{rg}}\right)^{n_w}$	Balancing simplicity and flexibility	Unclear physical mechanisms
Singh et al. (2019)	Gas phase: $k_{rg} = \frac{r_g^2}{R^2}\left[\alpha\left(1-\frac{r_w^2}{r_g^2}\right)-1\right]\frac{\tau(\phi,1-S_h-S_{wr})}{\tau(\phi,S_g)}$ Liquid phase: $k_{rw} = \frac{\left(r_w^2-r_g^2\right)^2}{R^2\left(r_w^2-r_g^2\right)}\frac{\tau(\phi,1-S_h-S_{wr})}{\tau(\phi,S_w)}$	Representing physical processes (pore-structure effects)	High complexity

(carried out in 2017 and 2020) (Wei et al., 2024; Wu et al., 2024a) (see Table 1).

As shown in Table 3, in the early-stage production tests, both the total cumulative productivity and the daily average productivity were low, but they exhibited a gradually increasing trend. They have uncovered some issues that are hard to identify in laboratory studies, such as the actual productivity being much lower than anticipated and sand production problems. The core problem lies in the insufficient comprehension of the gas-liquid multi-phase fluid migration during hydrate dissociation (see Table 2).

Currently, the economic viability of hydrate exploitation poses the most significant technical challenge. The depressurization method does not necessitate additional energy injection. Nevertheless, it will lead to a rapid decrease in the reservoir temperature, causing a sharp decline in gas production. The heat injection method will significantly reduce the overall energy efficiency of the exploitation process. The CO_2 replacement method has drawbacks such as slow CO_2 penetration and low replacement efficiency, and the produced gas contains a substantial amount of CO_2. Hence, perfecting the theoretical system of hydrate exploitation and substantially increasing the productivity on a magnitude scale are the keys to realizing the industrial production of hydrates.

5.2. Numerical simulation

Numerical simulation employs computers to formulate mathematical models for simulating the hydrate production process. Its advantages are manifested in relatively low cost, since it does not necessitate large-scale engineering operations on actual sites but merely relies on computer calculations. Furthermore, it can promptly simulate diverse situations under different production schemes, adjust and analyze multiple parameters within a short time frame, thereby enhancing research efficiency and facilitating the screening of more favorable production options. The challenge in applying this method resides in the requirement to comprehensively consider the flow behaviors of multi-phase fluids like water, gas, and hydrates within the intricate pore structures of sediments and to establish precise multi-phase flow models, with the aim of accurately predicting the dynamics production of fluids and the spatial evolution of the seepage field.

Based on on-site geological data from Canada's Mallik Delta, layered models incorporating permeability, porosity, and hydrate saturation heterogeneity were formulated (Xia et al., 2020; Lei et al., 2022b; Li et al., 2022c). Distinctive multi-phase flow behaviors in hydrate-bearing sediments during depressurization and heat injection decomposition processes were simulated and analyzed.

Long-term gas production of the Hydrate-01 well on Alaska's North Slope was investigated (Boswell et al., 2022). The impacts of different production well layouts and depressurization amplitudes on gas production under depressurization were delved into (Nakajima et al., 2022). A production approach for hydrate-bearing sediments in permafrost regions, combining depressurization and heat injection methods, was put forward (Wu et al., 2024a). The evolution of seepage parameters under different production schemes was analyzed, and the optimal production well configuration as well as production schemes for depressurization and heat injection were acquired (Moridis et al., 2024).

Based on geological data and the spatial distribution of production wells at the Nankai Trough hydrate production site in Japan, the spatially heterogeneous model was formulated. The Tough + Hydrate code was employed to analyze the

Table 3
Summary of global gas hydrate production tests.

Area	Canada			America	Japan		China			South China Sea	
	Mackenzie delta			North Slope of Alaska	Nankai Trough		Muli Basin				
Year	2002	2007	2008	2012	2013	2017	2011		2016	2017	2020
Production	Hot fluids	Depressurization		Depressurization + gas displacement	Depressurization		Depressurization + heat injection			Depressurization	
Production time	125 h	30 h	6 d	30 d	6 d	12 | 24 d	101 h		23 d	60 d	42 d
Cumulative productivity, m^3	516	830	1.3×10^4	2.4×10^4	1.2×10^5	2.0×10^5	95		1078.4	3.09×10^5	1.49×10^6
Daily productivity, m^3	99.9	664	2167	800	2×10^4	8330	22.57		46.87	5000	2.87×10^4
Stop reason	–	Sand production		–	Sand production | Initiative ending		–		–	Initiative ending	
Data sources	Hinz et al. (2019); Yang et al. (2019); Xu and Li (2024)			Luo et al. (2020); Chong et al. (2022); Zyrianova et al. (2024)	Ymamoto et al. (2019); Konno and Nagao (2021)		Meng et al. (2023); Pan and Schicks (2023); Han et al. (2024)			Ning et al. (2020); Ye et al. (2020); Li et al. (2023a); Li et al. (2023b)	

depressurization production process of sandy sediments via single vertical wells and complex structure wells, with the superiority of double-well synergistic productivity enhancement disclosed and optimization schemes for multi-branch horizontal well depressurization production put forward (Mao et al., 2023a; Xue et al., 2023; Xin et al., 2023). In response to severe sand production and blockage issues observed in two hydrate production tests, the independently developed gas-water-solid particle migration simulation program, HydrateSand, was applied to elucidate the abnormal phenomenon of premature gas production rate attenuation during the production process (Zhu et al., 2022; Qin et al., 2024b; An et al., 2025).

Based on the characteristics of interbedded mud-sand structures in India's Krishna Godavari Basin, the 3D model was formulated. Production capacity evaluations for depressurization production were conducted, the feasibility and production potential under different permeability conditions were appraised (Lijith et al., 2022; Zhang et al., 2024b), and gas production of multi-branch wells under varying geometric parameters (lateral branch inclination angles, numbers, and spacings) were deliberated (Xin et al., 2021a). Ultimately, it was deduced that with increasing permeability anisotropy, short-term gas and water production will augment, yet long-term methane production remains scarcely affected (Gong et al., 2022; Gandhi et al., 2024).

Based on seismic interpretation, logging curves, and core data from New Zealand's Pegasus Basin, the numerical simulation model incorporating microbial effects was formulated. Factors governing the distribution of hydrate reservoirs were studied (Pecher et al., 2024), the spatial trend of hydrate formation was forecasted (Kroeger et al., 2019), and hydrate resources were assessed (Chenin and Bedle, 2020).

Based on the geological conditions of the Shenhu Sea area in China, models for the two hydrate production tests were formulated (Sun et al., 2024b; Wan et al., 2024a, 2024b). The influence of the three-phase area was incorporated (Li et al., 2023d; Zang et al., 2024; Li, 2025); a production increase strategy combining multi-planar fractures with multi-sided well patterns and a formation method for the artificial CO_2 hydrate cap were put forward (Guo et al., 2024a, 2024b); the production increase effects of depressurization production by different horizontal well systems were deliberated (Zhang et al., 2021, 2022b; Chu et al., 2023); it was ascertained that the layout of radial pipes can effectively enhance productivity (Mahmood and Guo, 2023; Mao et al., 2023b; Jin et al., 2024); and it was noted that inclined strata result in decreased gas production and increased water production, with this phenomenon becoming more conspicuous as the inclination angle increases (Jin et al., 2021; Be et al., 2022; Qin et al., 2024a).

Regarding the study on accurately describing permeability evolution in hydrate exploitation simulation, Li et al. (2024a) investigated the Shenhu Sea hydrate production area in China using a systematic framework: First, a LBM model for multi-component multi-phase flow during hydrate decomposition was constructed to explore the mutual feedback mechanism between pore structure and permeability, and an "*S*-shaped" mathematical

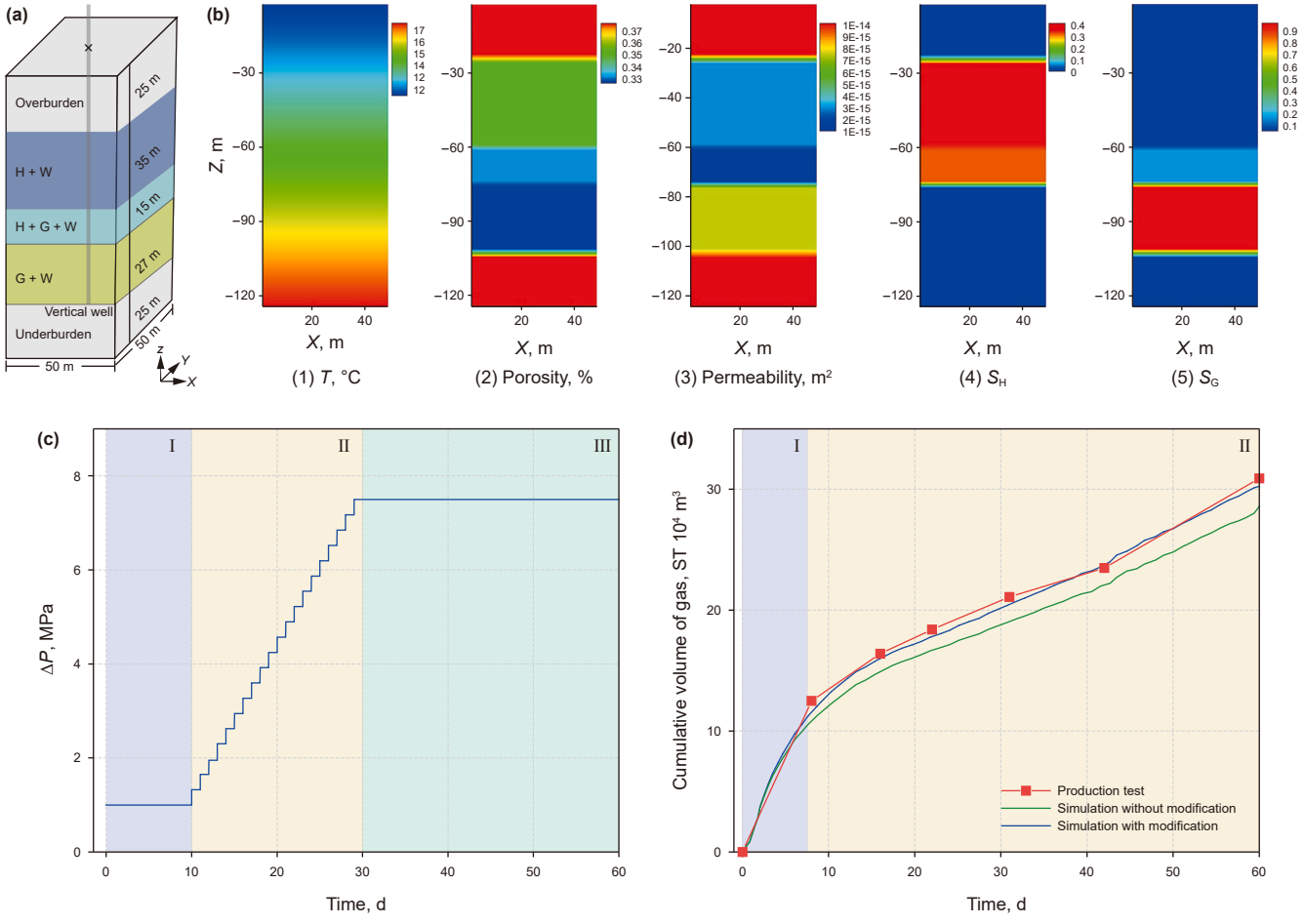

Fig. 5. Numerical simulation of the first marine gas hydrate production tests. **(a)** Conceptual hydrate production model; **(b)** initial condition; **(c)** simulation depressurization process; **(d)** comparison of gas production between the simulation results and the production test.

model describing the permeability evolution with hydrate saturation was established (Eq. (29)).

$$k_{\mathrm{nor}}(\%) = \frac{k(S_{\mathrm{h}})}{k_0} = 2.28826 + \frac{97.19184}{1 + \left(\frac{S_{\mathrm{h}}}{0.14732}\right)^{3.61664}} \tag{29}$$

Second, permeability of clayey silt cores under different hydrate saturations was measured using a self-developed multi-phase seepage system, and constant terms in the permeability model were determined. Third, numerical simulation programs integrating different permeability evolution models were developed based on the TOUGH + Hydrate code. Finally, application to China's first marine hydrate production test (Fig. 5) revealed that models with more accurate permeability evolution descriptions better explained field gas production dynamics, providing technical support for safe, efficient, and sustainable hydrate exploitation.

At the macroscopic scale, production tests and numerical simulations focus on predicting fluid migration and ensuring reservoir stability during hydrate exploitation. Global pilot tests provide field data on gas production dynamics and sand production, revealing productivity discrepancies stemming from inadequate multi-phase flow understanding. Numerical models simulate depressurization and thermal stimulation, optimizing well configurations and predicting seepage parameter evolution. Key challenges include accurately modeling geological heterogeneities, coupled thermo-hydro-mechanical processes, and economic viability, underscoring the need for multi-scale integration and real-time field data calibration to enable safe, efficient exploitation.

Therefore, the engineering significance of the permeability models in hydrate-bearing sediment can be succinctly summarized into three key aspects. Optimizing extraction strategies: Accurate models enhance gas production predictions and well configuration designs, thereby improving field recovery efficiency. Facilitating reservoir stability assessment: Models that capture dynamic pore structure changes help predict fluid migration and mitigate risks such as sand production during depressurization. Supporting economic viability analysis: Multi-scale models integrating core-scale experiments and numerical simulations optimize energy input and production schedules to balance technical feasibility with cost-effectiveness.

6. Conclusions and outlook

Presently, a substantial disparity exists between the gas productivity in hydrate production tests and the threshold for industrial production. Issues like sand production and blockage, the difficulty in depressurization arising from poor gas-water phase separation, and the surface subsidence in the early production stage have impeded safe and efficient exploitation. The crux of the matter resides in the ambiguous comprehension of the intricate problems related to the hydrate phase transition and the multi-phase flow of gas and water.

Numerous scholars have conducted a substantial amount of valuable work by employing a diverse range of technical means and have attained remarkable scientific achievements. Nevertheless, as research progresses further, there are still following issues that require intensified research:

(a) Inaccurate portrayal of the dynamic evolution characteristics of the pore structure during hydrate dissociation: In pore-scale simulations and core-scale experiments, hydrates within cores of varying saturation are predominantly generated uniformly and stochastically within the pore space, and the evolution of the pore structure concomitant with the decrease in hydrate saturation is discontinuous. Emerging technologies underutilized in the hydrate research field, such as microfluidic chip experiments, can enable controlled observation of hydrate nucleation and morphological transitions while precisely capturing the dynamic evolution of pore structures during hydrate dissociation.

(b) Ambiguous description of the gas and water multi-phase flow process within hydrate bearing sediments: The behavior of the gas and water phase fluid interfaces and the interaction mechanism have not been expounded upon in detail. The extant permeability evolution models have oversimplified the microscopic heterogeneous structure and the complex hydrate occurrence patterns, the relative permeability evolution models merely take into account the influence of gas and liquid phase saturation and fail to consider the dynamic feedback interaction between hydrate saturation and relative permeability. Consequently, the multi-phase seepage parameters utilized in site-scale simulations are static parameters and do not depict their dynamic evolution characteristics, thereby giving rise to poor applicability. Future models should integrate time-dependent variables (e.g., hysteresis) by resolving fluid–hydrate interactions through microscale simulations, incorporating saturation change rates into relative permeability models, and linking these to dynamic pore structure evolution to capture the dynamic feedback between hydrate saturation and seepage parameters

(c) Deficiency in multi-scale correlation and coupling: Studies on the permeability evolution during hydrate dissociation are preponderantly explored independently at each scale. Although certain individual studies have integrated the core scale and pore scale by means of CT technology, to begin with, there is a paucity of experimental samples, rendering it arduous to furnish detailed data requisite for mechanism analysis; furthermore, the actual circumstances of hydrate production tests have not been comprehensively taken into account, the research findings are challenging to be directly applied to actual production. To address this, the development of methods such as leveraging machine learning for multi-source data integration, developing CT-LBM cross-scale correlation models, creating multi-scale numerical frameworks, and incorporating field monitoring for dynamic calibration are necessary to bridge the scale gap.

CRediT authorship contribution statement

Yao-Bin Li: Writing – original draft, Writing – review & editing. **Xin Xin:** Writing – review & editing, Funding acquisition. **Hui-Xing Zhu:** Investigation, Validation. **Yue Su:** Funding acquisition. **Yi-Long Yuan:** Resources, Supervision. **Tian-Fu Xu:** Writing – review & editing, Funding acquisition.

Declaration of competing interest

The authors declare the following financial interests/personal relationships which may be considered as potential competing interests:There are no conflicts of interest of other works related to this paper.

Acknowledgments

This work was supported by the National Natural Science Foundation of China (No. 42276224, No. 3A2213285425 and No. 42206230).

References

Abdoli, S.M., Shafiei, S., Raoof, A., et al., 2018. Insight into heterogeneity effects in methane hydrate dissociation via pore–scale modeling. Trans. Porous Media 124, 183–201. https://doi.org/10.1007/s11242-018-1058-6.

Aghajanloo, M., Taghinejad, S.M., Voskov, D., et al., 2024. Influence of water saturation and water memory on CO_2 hydrate formation/dissociation in porous media under flowing condition. Chem. Eng. J. 492, 152455. https://doi.org/10.1016/j.cej.2024.152455.

An, Y., Zhang, Y.Q., Hui, C.Y., et al., 2025. Numerical simulation on natural gas hydrates exploitation via multilateral well: Impacts on sand production and geomechanical responses. Fuel 383, 133898. https://doi.org/10.1016/j.fuel.2024.133898.

Be, K.Q., Tian, H.L., Xu, T.F., et al., 2022. Effects of key geological factors in the long–term transport of CH_4 and the CH_4–hydrate formation behavior with formation dip. J. Nat. Gas Sci. Eng. 103, 104615. https://doi.org/10.1016/j.jngse.2022.104615.

Boswell, R., Collett, T.S., Yamamoto, K., et al., 2022. Scientific results of the Hydrate-01 stratigraphic test well program, Western Prudhoe Bay unit, Alaska North slope. Energy Fuels 36 (10), 5167–5184. https://doi.org/10.1021/acs.energyfuels.2c00327.

Cai, J.C., Qin, X.J., Xia, X.Z., et al., 2024. Numerical modeling of multiphase flow in porous media considering micro- and nanoscale effects: A comprehensive review. Gas Sci. Eng. 131, 205441. https://doi.org/10.1016/j.jgsce.2024.205441.

Cai, J.C., Xia, Y.X., Lu, C., et al., 2020a. Creeping microstructure and fractal permeability model of natural gas hydrate reservoir. Mar. Petrol. Geol. 115, 104282. https://doi.org/10.1016/j.marpetgeo.2020.104282.

Cai, J.C., Xia, Y.X., Xu, S., et al., 2020b. Advances in multi-phase seepage characteristics of natural gas hydrate sediments. Chin. J. Theor. Appl. Mech. 52 (1), 208–223. https://doi.org/10.6052/0459-1879-19-362.

Chen, Y., Yan, C.L., Cheng, Y.F., et al., 2024. DEM-CFD coupling verification and analysis of a sand control medium structure with weakened particle blockage performance. Powder Technol. 441, 119811. https://doi.org/10.1016/j.powtec.2024.119811.

Chenin, J.L., Bedle, H., 2020. Multi-attribute machine learning analysis for weak BSR detection in the Pegasus Basin, Offshore New Zealand. Mar. Geophys. Res. 41 (4), 21. https://doi.org/10.1007/s11001-020-09421-x.

Chong, L.B., Singh, H., Creason, C.G., et al., 2022. Application of machine learning to characterize gas hydrate reservoirs in Mackenzie Delta (Canada) and on the Alaska north slope (USA). Comput. Geosci. 26 (5), 1151–1165. https://doi.org/10.1007/s10596-022-10151-9.

Chu, H.Y., Zhang, J.X., Zhang, L.W., et al., 2023. A new semi–analytical flow model for multi–branch well testing in natural gas hydrates. Adv. Geo-Energy Res. 7 (3), 176–188. https://doi.org/10.46690/ager.2023.03.04.

Corey, A., 1986. Mechanics of Immiscible Fluids in Porous Media. Water Resources Publications. Colorado.

Dai, S., Seol, Y.K., 2014. Water permeability in hydrate–bearing sediments: a pore–scale study. Geophys. Res. Lett. 41 (12), 4176–4184. https://doi.org/10.1002/2014GL060535.

Delli, M., Grozic, J.L., 2013. Prediction performance of permeability models in gas–hydrate–bearing sands. SPE J. 182 (2), 274–284. https://doi.org/10.2118/149508-PA.

Deng, F.C., Wang, Y.F., Li, X.S., et al., 2024. A model-based study of the evolution of gravel layer permeability under the synergistic blockage effect of sand particle transport and secondary hydrate formation. Appl. Energy 355, 122209. https://doi.org/10.1016/j.apenergy.2023.122209.

Dong, L., Liu, X.Q., Gong, B., et al., 2024. Geomechanical properties of hydrate-bearing strata and their applications. Adv. Geo-Energy Res. 11 (3), 161–167. https://doi.org/10.46690/ager.2024.03.01.

Gambelli, A.M., 2023. Methane replacement into hydrate reservoirs with carbon dioxide: main limiting factors and influence of the gaseous phase composition, over hydrates, on the process. Chem. Eng. J. 478, 147–247. https://doi.org/10.1016/j.cej.2023.147247.

Gamwo, I.K., Liu, Y., 2010. Mathematical modeling and numerical simulation of methane production in a hydrate reservoir. Ind. Eng. Chem. Res. 49 (11), 5231–5245. https://doi.org/10.1021/ie901452v.

Gandhi, M., Khan, S.H., Arora, A., et al., 2024. Effect of isotropic and anisotropic permeability on gas production behavior of site NGHP-01-10D in Krishna-Godavari basin. Energies 17 (21), 5248. https://doi.org/10.3390/en17215248.

Gao, D.L., 2022. Focus on research advances in the natural gas hydrate resource evaluation: introduction to papers in the special section of evaluation of Natural gas hydrate resource potential in the South China Sea. Pet. Sci. 19 (1), 1–2. https://doi.org/10.1016/j.petsci.2023.08.027.

Ge, D.F., Zhang, J.C., Cao, Y.X., et al., 2024. Properties and model of pore-scale methane displacing water in hydrate-bearing sediments. J. Mar. Sci. Eng. 12 (8), 1320. https://doi.org/10.3390/jmse12081320.

Geranutti, B.L., Pohl, M., Rathmaier, D., et al., 2024. Multiphysics measurements for detection of gas hydrate formation in undersaturated oil coreflooding experiments with seawater injection. Energies 17 (13), 3280. https://doi.org/10.3390/en17133280.

Gong, G.J., Zhao, G.J., Pang, W.X., et al., 2023. Review of hydrate-bearing sediment permeability for natural gas hydrate exploitation: Measurement and application development. J. Petrol. Sci. Eng. 220 (B), 111217. https://doi.org/10.1016/j.petrol.2022.111217.

Gong, Y., Xu, T.F., Yuan, Y.L., et al., 2022. Optimal design of the field hydrate production test in the offshore India: Insights from the vertically heterogeneous hydrate reservoir model. J. Nat. Gas Sci. Eng. 103 (Suppl. C), 104645. https://doi.org/10.1016/j.jngse.2022.104645.

Gorenkov, I., Nikitin, V., Fokin, M., et al., 2024. Projection-subtraction X-ray imaging scheme for studying fast fluid-dynamics processes in porous media. Transport Porous Media 151 (3), 625–643. https://doi.org/10.1007/s11242-023-02055-8.

Gu, Y.H., Liu, X.J., Li, Y., et al., 2025. Feasibility analysis of liquid CO_2 injection and sequestration as hydrates in South China Sea marine sediments over 100 years. Appl. Energy 380, 125068. https://doi.org/10.1016/j.apenergy.2024.125068.

Guo, T.K., Wang, W.Y., Yang, X., et al., 2025. Numerical simulation of gravel packing in multi-branch horizontal wells in hydrate reservoirs based on CFD-DEM coupling. Geoenergy Sci. Eng. 244, 213445. https://doi.org/10.1016/j.geoen.2024.213445.

Guo, Y., Li, S.X., Huang, X., et al., 2024a. Numerical simulation and optimization of well parameters for depressurization–assisted CO_2 replacement using a PSO algorithm. Energy Fuels 38 (11), 9722–9733. https://doi.org/10.1021/acs.energyfuels.4c01313.

Guo, Y., Li, S.X., Sun, H., et al., 2024b. Enhancing gas production and CO_2 sequestration from marine hydrate reservoirs through optimized CO_2 hydrate cap. Energy 303, 131821. https://doi.org/10.1016/j.energy.2024.131821.

Han, Z.H., Li, R.R., Zhang, L.Q., et al., 2024. Multi-field coupling simulation of impact of temperature and density of heat injection well on carbon budget during hydrate exploitation in Qilian mountain permafrost region. J. Earth Sci. 35 (6), 1934–1943. https://doi.org/10.1007/s12583-023-1947-5.

Hinz, D., Arastoopour, H., Abbasian, J., 2019. A model for effective permeability in an unconsolidated hydrate reservoir. J. Nat. Gas Sci. Eng. 72, 103033. https://doi.org/10.1016/j.jngse.2019.103033.

Hu, C., Tian, Y.J., Liu, X.L., et al., 2024. Permeability of surface clay-bearing sediments in Shenhu Area of South China Sea. Eng. Geol. 335, 107535. https://doi.org/10.1016/j.enggeo.2024.107535.

Ji, Y.K., Kneafsey, T.J., Hou, J., et al., 2022. Relative permeability of gas and water flow in hydrate-bearing porous media: A micro-scale study by lattice Boltzmann simulation. Fuel 321, 124013. https://doi.org/10.1016/j.fuel.2022.124013.

Ji, Y.K., Hou, J., Zhao, E., et al., 2021. Pore-scale study on methane hydrate formation and dissociation in a heterogeneous micromodel. J. Nat. Gas Sci. Eng. 95, 104230. https://doi.org/10.1016/j.jngse.2021.104230.

Jiang, Y.J., Zhang, R.Q., Ye, R.J., et al., 2024. Mechanical properties of nodular natural gas hydrate-bearing sedimen. Adv. Geo-Energy Res. 11 (1), 41–53. https://doi.org/10.46690/ager.2024.01.05.

Jiao, X.H., He, W., Tian, Z.H., et al., 2025. Characterization of water microdistribution behavior in shale nanopores: a comparison between experiment and theoretical model. Adv. Geo-Energy Res. 15 (1), 79–86. https://doi.org/10.46690/ager.2025.01.08.

Jin, G.R., Liu, J., Liu, L.H., et al., 2021. Effect of lithological rhythm of a confined hydrate reservoir on gas production performance using water flooding in five–spot vertical well system. J. Nat. Gas Sci. Eng. 92, 104019. https://doi.org/10.1016/j.jngse.2021.104019.

Jin, G.R., Liu, J., Su, Z., et al., 2024. Gas production from a promising reservoir of the hydrate with associated and shallow gas layers in the low permeable sediments. Energy 295, 131079. https://doi.org/10.1016/j.energy.2024.131079.

Katagiri, J., Konno, Y., Yoneda, J., et al., 2017. Pore–scale modeling of flow in particle packs containing grain–coating and pore–filling hydrates: Verification of a Kozeny–Carman–based permeability reduction model. J. Nat. Gas Sci. Eng. 45, 537–551. https://doi.org/10.1016/j.jngse.2017.06.019.

Kleinberg, R.L., Flaum, C., Griffin, D.D., et al., 2003. Deep sea NMR: Methane hydrate growth habit in porous media and its relationship to hydraulic permeability, deposit accumulation, and submarine slope stability. J. Geophys. Res. Solid Earth 108 (B10), 2508. https://doi.org/10.1029/2003JB002389.

Konno, Y., Nagao, Y., 2021. Methane hydrate in marine sands: Its reservoir properties, gas production behaviors, and enhanced recovery methods. J. Jpn. Petrol. Inst. 64 (3), 113–122. https://doi.org/10.1627/jpi.64.113.

Kou, X., Zhang, H., Li, X.S., et al., 2024. Methane hydrate phase transition in marine clayey sediments: enhanced structure change and solid migration. Appl. Energy 368, 123485. https://doi.org/10.1016/j.apenergy.2024.123485.

Krishna, S., Mahant, B.K., Robustillo, M.D., et al., 2024. The role of gas hydrates in storing natural gas-hydrogen blends for coupling Power-to-X and decarbonization. Energy Fuels 38 (24), 23192–23229. https://doi.org/10.1021/acs.energyfuels.4c03950.

Kroeger, K.F., Crutchley, G.J., Kellett, R., et al., 2019. A 3–D model of gas generation, migration, and gas hydrate formation at a young convergent margin (Hikurangi margin, New Zealand). G-cubed 20 (11), 5126–5147. https://doi.org/10.1029/2019GC008275.

Lei, L., Park, T.Y., Jarvis, K., et al., 2022a. Pore–scale observations of natural hydrate–bearing sediments via pressure core sub–coring and micro–CT scanning. Sci. Rep. 12 (1), 1–17. https://doi.org/10.1038/s41598-022-07184-6.

Lei, J., Guo, W., Yang, X., et al., 2024. Parameters optimization of storage capacity of hole-bottom freezing sampling technique for natural gas hydrates. Adv. Geo-Energy Res. 12 (1), 66–76. https://doi.org/10.46690/ager.2024.04.06.

Lei, H.W., Yang, Z.J., Xia, Y.L., et al., 2022b. Prospects of gas production from the vertically heterogeneous hydrate reservoirs through depressurization in the Mallik site of Canada. Energy Rep. 8, 2273–2287. https://doi.org/10.1016/j.egyr.2022.01.170.

Lei, X., Yao, Y.B., Luo, W.J., et al., 2021. Permeability change in hydrate bearing sediments as a function of hydrate saturation: A theoretical and experimental study. J. Petrol. Sci. Eng. 208 (PartB), 109449. https://doi.org/10.1016/j.petrol.2021.109449.
Li, G., Li, X.S., Lv, Q.N., et al., 2019. Permeability measurements of quartz sands with methane hydrate. Chem. Eng. Sci. 1, 1–5. https://doi.org/10.1016/j.ces.2018.08.055.
Li, G., Xu, Z.L., Li, X.S., et al., 2021. Permeability investigation and hydrate migration of hydrate−bearing silty sands and silt. J. Nat. Gas Sci. Eng. 89, 103891. https://doi.org/10.1016/j.jngse.2021.103891.
Li, X.X., Cui, W., Ma, T., et al., 2023a. Lattice Boltzmann simulation of coupled depressurization and thermal decomposition of carbon dioxide hydrate for cold thermal energy storage. Energy 278 (B), 127984. https://doi.org/10.1016/j.energy.2023.127984.
Li, Y.B., 2025. Dynamic Evolution of Multi-phase Seepage Parameters During Hydrate Dissociation in Clayey Silt Sediments PhD dissertation Jilin University, Changchun, Jilin CN. https://doi.org/10.27162/d.cnki.gjlin.2025.000813 (in Chinese).
Li, Y.B., Xin, X., Liu, M.W., et al., 2025. An experimental study on gas-liquid phase fluid migration in hydrate-bearing sediments during hydrate dissociation. Eng. Geol. 354, 108163. https://doi.org/10.1016/j.enggeo.2025.108163.
Li, Y.B., Xin, X., Xu, T.F., et al., 2023a. Production behavior of hydrate−bearing sediments with mixed fracture− and pore−filling hydrates. J. Mar. Sci. Eng. 11 (7), 1321. https://doi.org/10.3390/jmse11071321.
Li, Y.B., Xin, X., Xu, T.F., et al., 2023b. Study of multibranch wells for productivity increase in hydrate reservoirs based on a 3D heterogeneous geological model: a case in the Shenhu Area, South China Sea. SPE J. 28 (5), 2207–2222. https://doi.org/10.2118/215814-PA.
Li, Y.B., Xin, X., Xu, T.F., et al., 2022a. Comparative analysis on the evolution of seepage parameters in methane hydrate production under depressurization of clayey silt reservoir and sandy reservoir. J. Mar. Sci. Eng. 10 (653), 653. https://doi.org/10.3390/jmse10050653.
Li, Y.B., Xu, T.F., Xin, X., et al., 2022b. Study on gas hydrate reservoir reconstruction for enhanced gas production in Shenhu area of the South China Sea based on 3D heterogeneous geological model. Energy Fuels 36, 12695–12707. https://doi.org/10.1021/acs.energyfuels.2c02549.
Li, Y.B., Xu, T.F., Xin, X., et al., 2024a. Multi-scale comprehensive study of the dynamic evolution of permeability during hydrate dissociation in clayey silt hydrate-bearing sediments. Adv. Geo-Energy Res. 12 (2), 127–140. https://doi.org/10.46690/ager.2024.05.05.
Li, Y.B., Xu, T.F., Xin, X., et al., 2024b. Pore-scale study of the dynamic evolution of multi-phase seepage parameters during hydrate dissociation in clayey silt hydrate-bearing sediments. J. Hydrol. 635, 131178. https://doi.org/10.1016/j.jhydrol.2024.131178.
Li, Y.B., Xu, T.F., Xin, X., et al., 2024c. Optimization of gas production from hydrate−bearing sediments with fluctuated characteristics. J. Ocean Univ. China 23 (3), 618–632. https://doi.org/10.1007/s11802-024-5633-x.
Li, Y.B., Xu, T.F., Xin, X., et al., 2024d. Effects of dipping and folded structure on gas production from hydrate-bearing sediments. SPE J. 29 (2), 1129–1146. https://doi.org/10.2118/217991-PA.
Li, Y.B., Xu, T.F., Xin, X., et al., 2023c. Sensitivity analysis of multi−phase seepage parameters affecting the clayey silt hydrate reservoir productivity in the Shenhu Area. Acta Geol. Sin. 97 (6), 1787–1800. https://doi.org/10.1111/1755-6724.15106.
Li, Y.H., Huang, L., Wu, P., et al., 2024e. Investigation on multi−parameter of hydrate−bearing synthetic sediment during hydrate replacement process: a in−situ X−ray computed tomography study. Sci. Total Environ. 929, 172621. https://doi.org/10.1016/j.scitotenv.2024.172621.
Li, Y.H., Shang, A.R., Wu, C.A., et al., 2024f. Permeability anisotropy of hydrate-bearing sediment during consolidation process: Insights from CT scanning and Pore Network modeling. Energy Fuels 38 (7), 5900–5913. https://doi.org/10.1021/acs.energyfuels.4c00102.
Li, Y.H., Wei, Z.S., Zhang, K., et al., 2024g. Experimental study on the impact of effective stress and cyclic loading on permeability of methane hydrate clayey sediments. Gas Sci. Eng. 124, 205282. https://doi.org/10.1016/j.jgsce.2024.205282.
Li, Y.L., Ning, F.L., Xu, M., et al., 2023c. Experimental study on solid particle migration and production behaviors during marine natural gas hydrate dissociation by depressurization. Pet. Sci. 30 (6), 3610–3623. https://doi.org/10.1016/j.petsci.2023.05.018.
Li, Z.R., Zhao, L.S., Cao, Z.J., et al., 2024h. Application of coupled hydrodynamic and thermal Lattice-Boltzmann simulation on permeability estimation of hydrate-bearing sediment during hydrate dissociation processes. Geoenergy Sci. Eng. 241, 213066. https://doi.org/10.1016/j.geoen.2024.213066.
Li, Z., Spangenberg, E., Schicks, J.M., et al., 2022c. Numerical simulation of coastal sub-permafrost gas hydrate formation in the Mackenzie Delta, Canadian arctic. Energies 15 (14), 4986. https://doi.org/10.3390/en15144986.
Li, Z.Y., Wang, Z.Y., Ji, H.F., 2024i. Parameters variation of natural gas hydrate with thermal fluid dissociation based on multi-field coupling under pore-scale modeling. Water 16 (19), 2734. https://doi.org/10.3390/w16192734.
Lijith, K.P., Srinivasa, R.R., Narain, S.D., 2022. Investigations on the influence of wellbore configuration and permeability anisotropy on the gas production from a turbidite hydrate reservoir of KG Basin. Fuel 317, 123562. https://doi.org/10.1016/j.fuel.2022.123562.
Liu, M.W., 2024. Clay-Dominant Geomaterials: From Suspensions to Shales. PhD dissertation. Georgia Institute of Technology, Atlanta, Georgia, US.
Liu, W.G., Chen, Y.K., Shang, A.R., et al., 2024. Permeability anisotropy analysis of two-phase flow during hydrate dissociation process. Gas Sci. Eng. 126, 205342. https://doi.org/10.1016/j.jgsce.2024.205342.
Liu, X.H., Zhang, J.D., Bhawangirkar, D.R., et al., 2024a. Effect of particle size distribution variability on the permeability of hydrate−bearing sediments: A CFD study. Gas Sci. Eng. 126, 205335. https://doi.org/10.1016/j.jgsce.2024.205335.
Liu, X.L., Jia, Y.G., Zhang, J.W., et al., 2017. An experimental investigation of wave-induced sediment responses in a natural silty seabed: New insights into seabed stratification. Sedimentology 67 (2), 508–529. https://doi.org/10.1111/sed.12312.
Liu, X.L., Lu, Y., Yu, H.Y., et al., 2022. In-situ observation of storm-induced wave-supported fluid mud occurrence in the subaqueous Yellow River Delta. J. Geophys. Res.: Oceans 127 (7), e2021JC018190. https://doi.org/10.1029/2021JC018190.
Liu, X.L., Wang, Y.Y., Zhang, H., et al., 2023. Susceptibility of typical marine geological disasters: An overview. Geoenviron. Disast. 10 (1), 1–13. https://doi.org/10.1186/s40677-023-00237-6.
Liu, X.Q., Han, Z.X., Luo, Z.L., et al., 2024b. Sand control mechanism of radial well filled with phase change material in hydrate reservoir. Pet. Sci. 21 (4), 2571–2582. https://doi.org/10.1016/j.petsci.2024.04.008.
Lu, C., Qin, X., Sun, J.S., et al., 2023. Research progress and scientific challenges in the depressurization exploitation mechanism of clayey-silt natural gas hydrates in the northern South China Sea. Adv. Geo-Energy Res. 10 (1), 14–20. https://doi.org/10.46690/ager.2023.10.03.
Lu, C., Xia, Y.X., Sun, X.,X., et al., 2019. Permeability evolution at various pressure gradients in natural gas hydrate reservoir at the Shenhu area in the South China Sea. Energies 12 (19), 3688. https://doi.org/10.3390/en12193688.
Luo, T.T., Li, Y.H., Madhusudhan, B.N., et al., 2020. Comparative analysis of the consolidation and shear behaviors of CH_4 and CO_2 hydrate-bearing silty sediments. J. Nat. Gas Sci. Eng. 75, 103157. https://doi.org/10.1016/j.jngse.2020.103157.
Luo, Y.J., Sun, Y.S., Li, L.J., et al., 2022. Image-based pore-network modeling of two-phase flow in hydrate-bearing porous media. Energy 252, 124044. https://doi.org/10.1016/j.energy.2022.124044.
Mahmood, M.N., Guo, B.Y., 2023. Gas production from marine gas hydrate reservoirs using geothermal−assisted depressurization method. Adv. Geo-Energy Res. 7 (2), 90–98. https://doi.org/10.46690/ager.2023.02.03.
Mahabadi, N., Jang, J.W., 2014. Relative water and gas permeability for gas production from hydrate−bearing sediments. G-cubed 15 (6), 2346–2353. https://doi.org/10.1002/2014GC005331.
Mao, P.X., Wu, N.Y., Ning, F.L., et al., 2023a. Gas production from muddy hydrate reservoirs by a spiral multilateral well network: effects of well deployment and production methods. Gas Sci. Eng. 118, 205087. https://doi.org/10.1016/j.jgsce.2023.205087.
Mao, P.X., Wu, N.Y., Wan, Y.Z., et al., 2023b. Optimization of a multi−fractured multilateral well network in advantageous structural positions of ultralow−permeability hydrate reservoirs. Energy 268, 126623. https://doi.org/10.1016/j.energy.2023.126623.
Masuda, Y., 1997. Numerical caculation of gas production performance from reservoirs containing natural gas hydrates. In: Proceedings of the Annual Technical Conference. San Antonio, Texas.
Meng, Q.G., Liu, C.L., Lu, Z.Q., et al., 2023. Growth behavior and resource potential evaluation of gas hydrate in core fractures in Qilian Mountain permafrost area, Qinghai-Tibet Plateau. China Geol. 6 (2), 208–215. https://doi.org/10.31035/cg2023021.
Meng, X.S., Liu, X.L., Wang, Y.Y., et al., 2024. Submarine landslide susceptibility assessment integrating frequency ratio with supervised machine learning approach. Appl. Ocean Res. 453, 104237. https://doi.org/10.1016/j.apor.2024.104237.
Moridis, G.J., 1998. EOSHYDR: A TOUGH2 module for CH_4−hydrate release and flow in the subsurface. Methane Hydrates. Chiba, Japan.
Moridis, G.J., Kim, J., Reagan, M.T., et al., 2023. Analysis of short- and long-term system response during gas production from a gas hydrate deposit at the UBGH2-6 site of the Ulleung Basin in the Korean East Sea. Can. J. Chem. Eng. 101 (2), 735–763. https://doi.org/10.1002/cjce.24626.
Moridis, G.J., Reagan, M.T., Huang, T.J., 2024. Numerical simulations in support of a long-term test of gas production from hydrate accumulations on the Alaska North Slope: water production and associated design and management issuesa. Energy Fuels 38 (14), 12824–12854. https://doi.org/10.1021/acs.energyfuels.4c01826.
Nakajima, C., Ouchi, H., Tamaki, M., et al., 2022. Sensitivity and uncertainty analysis for natural gas hydrate production tests in Alaska. Energy Fuels 36 (14), 7434–7455. https://doi.org/10.1021/acs.energyfuels.2c00335.
Ning, F.L., Liang, J.Q., Wu, N.Y., et al., 2020. Reservoir characteristics of natural gas hydrates in China. Nat. Gas. Ind. 40 (8), 1–24. https://doi.org/10.3787/j.issn.1000-0976.2020.08.001. (in Chinese).
Ohtsuki, S., Gao, B., Yoshii, T., et al., 2024. First successful wireline stress testing in a gas hydrate reservoir in the Hyuganada Sea, Japan. Energies 17 (1), 2610. https://doi.org/10.3390/en17112610.
Pan, M.D., Schicks, J.M., 2023. Unraveling the role of natural sediments in sII mixed gas hydrate formation: An experimental study. Molecules 28 (15), 5887. https://doi.org/10.3390/molecules28155887.
Parisa, N., Manja, L.H., Judith, M.S., 2024. Dissociation behavior of sI and sII gas hydrates in response to environmental changes-Investigations on the self-preservation effect. Appl. Energy 374, 124042. https://doi.org/10.1016/j.apenergy.2024.124042.

Pecher, I.A., Kroeger, K.F., Crutchley, G.J., et al., 2024. Gas hydrate stability for CO_2-methane gas mixes in the Pegasus Basin, New Zealand: A geological control for potential gas production using methane-CO_2 exchange in hydrate. Gas Sci. Eng. 131, 205456. https://doi.org/10.1016/j.jgsce.2024.205456.

Peng, H., Li, X.S., Chen, Z.Y., et al., 2024. Effect of gravel pack permeability on horizontal well productivity loss under secondary methane hydrate Formation: Experimental optimization of 3D randomly distributed mixed sand pack. Appl. Energy 371, 123663. https://doi.org/10.1016/j.apenergy.2024.123663.

Qin, F.F., Sun, J.X., Guo, Y.H., et al., 2024a. Numerical simulation on production trials by using depressurization for typical marine hydrate reservoirs: well type and formation dip. J. Ocean Univ. China 23 (3), 661–675. https://doi.org/10.1007/s11802-024-5566-4.

Qin, S.B., Sun, J.X., Liu, T.L., et al., 2024b. Sand control during gas production from marine hydrate reservoirs by using microbial-induced carbonate precipitation technology: A feasibility study. Energy 299, 131494. https://doi.org/10.1016/j.energy.2024.131494.

Ren, J.J., Yin, Z.Y., Chen, G.J., et al., 2024. Effect of marine clay minerals on the thermodynamics of CH_4 hydrate: Evidence for the inhibition effect with implications. Chem. Eng. J. 488, 151148. https://doi.org/10.1016/j.cej.2024.151148.

Ren, X.W., Guo, Z.Y., Ning, F.L., et al., 2020. Permeability of hydrate-bearing sediments. Earth Sci. Rev. 202, 103100. https://doi.org/10.1016/j.earscirev.2020.103100.

Sakurai, S., Aman, Z.M., Nonoue, T., et al., 2024. Simulations of hydrate reformation in the water production line of the second offshore methane hydrate production test in Japan's Nankai trough. Fuel 349, 128606. https://doi.org/10.1016/j.fuel.2023.128606.

Singh, H., Myshakin, E.M., Seol, Y.K., 2019. A nonempirical relative permeability model for hydrate–bearing sediments. SPE J. 24 (2), 547–562. https://doi.org/10.2118/193996-PA.

Song, H.M., Zhao, J.Z., Yin, Z.Y., et al., 2024a. Experimental study on metastable dissociation of sandy hydrate reservoirs. Chem. Eng. Sci. 286, 119685, 0.101610.1016/j.ces.2023.119685.

Song, Y.Q., Zhang, D.C., Ranjith, P.G., et al., 2024b. A comprehensive study of fines migration in internally unstable natural gas hydrate reservoirs. Powder Technol. 433, 119193. https://doi.org/10.1016/j.powtec.2023.119193.

Sun, J.S., Li, Y.Y., Liao, B., et al., 2024a. Development and performance evaluation of bioenzyme-responsive temporary plugging materials. Adv. Geo-Energy Res. 11 (1), 20–28. https://doi.org/10.46690/ager.2024.01.03.

Sun, J.X., Guo, Y.H., Yin, Z.Y., et al., 2024b. Production performance of multiple approaches for stimulating the layered hydrate reservoir with high permeability under horizontal well systems. Ocean Eng. 303, 117781. https://doi.org/10.1016/j.oceaneng.2024.117781.

Sun, Z.Y., Huang, H.K., Jiao, K.T., et al., 2025. Thermal-hydraulic-mechanical-chemical multiphysics coupling for geothermal energy development. Adv. Geo-Energy Res. 16 (2), 91–94. https://doi.org/10.46690/ager.2025.05.01.

Tamaki, M., Fujimoto, A., Boswell, R., et al., 2022. Geological reservoir characterization of a gas hydrate prospect associated with the hydrate–01 stratigraphic test well, Alaska North Slope. Energy Fuels 36 (15), 8128–8149. https://doi.org/10.1021/acs.energyfuels.2c00336.

Tian, H.T., Liu, L.L., Zhu, L.Q., et al., 2023. Relationship between normalized permeability and resistivity index in hydrate–bearing sediments: fractal model and numerical simulation. Geophys. J. Int. 234 (1), 684–698. https://doi.org/10.1093/gji/ggad090.

Van, G., 1980. A closed–form equation for predicting the hydraulic conductivity of unsaturated soils. Soil Sci. Soc. Am. J. 44 (5), 892–898. https://doi.org/10.2136/sssaj1980.03615995004400050002x.

Wan, T.H., Li, Z.Z., Wen, M.M., et al., 2024a. Numerical simulation of production behavior with different complex structure well types in Class 1–type hydrate reservoir. J. Mar. Sci. Eng. 12 (3), 508. https://doi.org/10.3390/jmse12030508.

Wan, T.H., Yu, M., Lu, H.F., et al., 2024b. Numerical simulation of vertical well depressurization with different deployments of radial laterals in Class 1–type hydrate reservoir. Energies 17 (5), 1139. https://doi.org/10.3390/en17051139.

Wang, H.J., Li, Y.H., Huang, L., et al., 2024a. A pore-scale study on microstructure and permeability evolution of hydrate-bearing sediment during dissociation by depressurization. Fuel 358 (A), 130124. https://doi.org/10.1016/j.fuel.2023.130124.

Wang, L., Shen, S., Wu, Z., et al., 2024b. Strength and creep characteristics of methane hydrate-bearing clayey silts of the South China Sea. Energy 294, 130789. https://doi.org/10.1016/j.energy.2024.130789.

Wang, S., Catherine, S., Tom, B., 2023. Pore–scale imaging of multiphase flow fluctuations in continuum–scale samples. Water Resour. Res. 59 (6), e2023WR034720. https://doi.org/10.1029/2023WR034720.

Wang, T., Chen, S.H., Li, M.L., et al., 2024c. A resolved CFD-DEM investigation of near-wellbore fine sand migration and production during methane hydrate extraction. Geomechan. Energy Environ. 38, 100561. https://doi.org/10.1016/j.gete.2024.100561.

Wang, Z.H., Wan, Y.Z., Zhang, Y.C., et al., 2024d. Gas and water relative permeability in THF hydrate-bearing Berea sandstone. Energy Fuels 38 (13), 11706–11716. https://doi.org/10.1021/acs.energyfuels.4c01402.

Wei, N., Pei, J., Li, H.T., et al., 2024. Classification of natural gas hydrate resources: review, application and prospect. Gas Sci. Eng. 124, 205269. https://doi.org/10.1016/j.jgsce.2024.205269.

Wu, C., Xin, X., Xu, T.F., et al., 2024a. Numerical simulation of natural gas hydrates production on the Alaska North Slope under depressurization combined with thermal stimulation. Energy Fuels 38 (24), 23519–23534. https://doi.org/10.1021/acs.energyfuels.4c04766.

Wu, N.Y., Li, Y.L., Wan, Y.Z., et al., 2020. Prospect of marine natural gas hydrate stimulation theory and technology system. Nat. Gas. Ind. 40 (8), 100–115.

Wu, P., Chen, Y.K., Shang, A.R., et al., 2024b. Anisotropy analysis of two–phase flow permeability in the multi–stage shear process of hydrate–bearing sediments. Energy 293, 130697. https://doi.org/10.1016/j.energy.2024.130697.

Wu, P., Li, Y.H., Wang, L., et al., 2022a. Hydrate-bearing sediment of the South China Sea: microstructure and mechanical characteristics. Eng. Geol. 307, 106782. https://doi.org/10.1016/j.enggeo.2022.106782.

Wu, Z.R., Yang, S.H., Liu, W.G., et al., 2022b. Experimental study on the difference of fluid flow between methane hydrate–bearing sand and clay sediments. Energy Fuels 36 (5), 2739–2750. https://doi.org/10.1021/acs.energyfuels.1c04155.

Xia, Y.L., 2022. Multi-Scale Joint Study on Dynamic Evolution Characteristics of Reservoir Seepage Parameters During Hydrate Dissociation. PhD dissertation. Jilin University, Changchun, Jilin. https://doi.org/10.27162/d.cnki.gjlin.2022.000241. CN (Sep. 2022.

Xia, Y.L., Xu, T.F., Yuan, Y.L., et al., 2020. Effect of perforation interval design on gas production from the validated hydrate-bearing deposits with layered heterogeneity by depressurization. Geofluids 2020, 8833884. https://doi.org/10.1155/2020/8833884.

Xia, Y.X., Elsworth, D., Cai, J.C., et al., 2024. Pore–scale water–gas distribution and gas permeability of natural gas hydrate reservoirs in the South China Sea. Geosci. Front. 15 (4), 101816. https://doi.org/10.1016/j.gsf.2024.101816.

Xia, Y.X., Xu, S., Lu, C., et al., 2023. Characterization and capillary pressure curve estimation of clayey-silt sediment in gas hydrate reservoirs of the South China Sea. Adv. Geo-Energy Res. 10 (3), 200–207, 0.46690/ager.2023.12.06.

Xin, X., Li, S., Xu, T.F., et al., 2021a. Numerical investigation on gas production performance in methane hydrate of multilateral well under depressurization in Krishna–Godavari Basin. Geofluids 2021, 9936872. https://doi.org/10.1155/2021/9936872.

Xin, X., Shan, Y., Xu, T.F., et al., 2023. Multi–lateral well productivity evaluation based on three–dimensional heterogeneous model in Nankai Trough, Japan. Energies 16 (5), 16052406. https://doi.org/10.3390/en16052406.

Xin, X., Yang, B., Xu, T.F., et al., 2021b. Effect of hydrate on gas/water relative permeability of hydrate–bearing sediments: pore–scale microsimulation by the Lattice Boltzmann Method. Geofluids 2021, 1396323. https://doi.org/10.1155/2021/1396323.

Xu, J.C., Bu, Z.W., Qin, H.T., et al., 2023a. Pore-scale modeling of seepage behaviors and permeability evolution in heterogeneous hydrate-bearing sediments and its implications for the permeability model. Geoenergy Sci. Eng. 221, 211372. https://doi.org/10.1016/j.geoen.2022.211372.

Xu, R., Kou, X., Wu, T.W., et al., 2023b. Pore-scale experimental investigation of the fluid flow effects on methane hydrate formation. Energy 271, 126967. https://doi.org/10.1016/j.energy.2023.126967.

Xu, Z.Q., Li, Y., 2024. Effect of skeleton grain size on the saturation of gas hydrate in natural sediments. J. Ocean Univ. China 23 (3), 676–682. https://doi.org/10.1007/s11802-024-5579-z.

Xue, K.P., Liu, Y., Yu, T., et al., 2023. Numerical simulation of optimized step–wise depressurization for enhanced natural gas hydrate production in the Nankai Trough of Japan. Processes 11 (6), 1812. https://doi.org/10.3390/pr11061812.

Yang, B., Xu, T.F., Du, Y.L., et al., 2024a. Numerical investigation on the influence of CO_2-induced mineral dissolution on hydrogeological and mechanical properties of sandstone using coupled lattice Boltzmann and finite element model. J. Hydrol. 639, 131616. https://doi.org/10.1016/j.jhydrol.2024.131616.

Yang, J.Y., Dai, X.Y., Xu, Q.H., et al., 2021. Pore–scale study of multicomponent multiphase heat and mass transfer mechanism during methane hydrate dissociation process. Chem. Eng. J. 423 (0), 130206. https://doi.org/10.1016/j.cej.2021.130206.

Yang, J.Y., Liu, Y.Z., Xu, Q.H., et al., 2024b. Pore-scale visualization of hydrate dissociation and mass transfer during depressurization using microfluidic experiments. Fuel 368, 131519. https://doi.org/10.1016/j.fuel.2024.131519.

Yang, J.Y., Xu, Q.H., Liu, Z.Y., et al., 2022. Pore-scale study of the multiphase methane hydrate dissociation dynamics and mechanisms in the sediment. Chem. Eng. J. 430 (2), 132786. https://doi.org/10.1016/j.cej.2021.132786.

Yang, L., Liu, Y.L., Zhang, H.Q., et al., 2019. The status of exploitation techniques of natural gas hydrate. Chin. J. Chem. Eng. 27 (9), 2133–2147.

Ye, J.L., Qin, X.W., Xie, W.W., et al., 2020. The second natural gas hydrate production test in the South China Sea. China Geol. 2, 197–209. https://doi.org/10.31035/cg2020043.

Ymamoto, K., Wang, X.X., Tamak, M., et al., 2019. The second offshore production of methane hydrate in the Nankai Trough and gas production behavior from a heterogeneous methane hydrate reservoir. RSC Adv. 9, 25987–26013. https://doi.org/10.1039/c9ra00755e.

Yoneda, J., Oshima, M., Kida, M., et al., 2019. Permeability variation and anisotropy of gas hydrate–bearing pressure–core sediments recovered from the Krishna–Godavari Basin, offshore India. Mar. Petrol. Geol. 108, 524–536. https://doi.org/10.1016/j.marpetgeo.2018.07.006.

You, Z.S., Hao, Y., Hu, W.K., et al., 2023. Strength analysis of hydrate-bearing sandy sediments in excess gas and excess water based on drained triaxial compression tests. Eng. Geol. 325, 107292. https://doi.org/10.1016/j.enggeo.2023.107292.

Yuan, X.L., Shi, B.C., Zhan, C.J., et al., 2022. A phase–field–based lattice Boltzmann model for multiphase flows involving N immiscible incompressible fluids. Phys. Fluids 34 (2), 1–14. https://doi.org/10.1063/5.0078507.

Zang, Y.Q., Xin, X., Xu, T.F., et al., 2024. Comparative study on improving the production of Class 1 and Class 3 reservoirs by using enlarged permeable well wall technology. Energy Fuels 38 (7), 5862–5880. https://doi.org/10.1021/acs.energyfuels.3c05046.

Zhang, A.Y., Cai, M., Wei, N., et al., 2024a. Analysis of sensitivity to hydrate blockage risk in natural gas gathering pipeline. Pet. Sci. 21 (4), 2723–2733. https://doi.org/10.1016/j.petsci.2024.01.016.

Zhang, J.C., Moridis, G.J., Blasingame, T.A., 2024b. Field-scale numerical investigation of a hybrid gas production method from the oceanic hydrate accumulation at site NGHP-02-09 in the Krishna-Godavari Basin, and the associated geomechanical responses. Mar. Petrol. Geol. 164, 106792. https://doi.org/10.1016/j.marpetgeo.2024.106792.

Zhang, J.D., Liu, X.H., Chen, D.Y., et al., 2022a. An investigation on the permeability of hydrate−bearing sediments based on pore−scale CFD simulation. Int. J. Heat Mass Tran. 192, 122901. https://doi.org/10.1016/j.ijheatmasstransfer.2022.122901.

Zhang, J.D., Song, Z.Y., Zhou, K.G., et al., 2024c. Pore-scale analysis of the permeability and effective thermal conductivity of hydrate-bearing sediments based on a high-pressure microfluidics approach. Energy Fuels 38 (22), 22192–22204. https://doi.org/10.1021/acs.energyfuels.4c04411.

Zhang, J.D., Yin, Z.Y., Li, Q.P., et al., 2023. Comparison of fluid production between excess−gas and excess−water hydrate−bearing sediments under depressurization and its implication on energy recovery. Energy 282, 128315. https://doi.org/10.1016/j.energy.2023.128315.

Zhang, J.D., Yin, Z.Y., Li, Q.P., et al., 2024d. An investigation on CH_4 hydrate transition and gas bubble evolution on a microfluidic chip. Chin. J. Theor. Appl. Mech. 56 (6), 1615–1623.

Zhang, J.D., Yin, Z.Y., Khan, S.A., et al., 2024e. Path-dependent morphology of CH_4 hydrates and their dissociation studied with high-pressure microfluidics. Lab Chip 24 (6), 1602–1615. https://doi.org/10.1039/d3lc00950e.

Zhang, P.P., Tian, S.C., Zhang, Y.Q., et al., 2021. Numerical simulation of gas recovery from natural gas hydrate using multi−branch wells: A three−dimensional model. Energy 220, 119549. https://doi.org/10.1016/j.energy.2020.119549.

Zhang, P.P., Zhang, Y.Q., Zhang, W.H., et al., 2022b. Numerical simulation of gas production from natural gas hydrate deposits with multi−branch wells: Influence of reservoir properties. Energy 238 (B), 1121738. https://doi.org/10.1016/j.energy.2021.121738.

Zhang, Y.C., Li, C.S., Ma, J.F., et al., 2022c. Investigating the effective permeability evolution as a function of hydrate saturation in the hydrate-bearing sands using a kinetic-theory-based pore network model. Comput. Geotech. 150, 104930. https://doi.org/10.1016/j.compgeo.2022.104930.

Zhang, Z., Li, Z.K., Li, C.F., et al., 2024f. Analysis of permeability anisotropy of marine hydrate-bearing sediments using fractal theory combined with X-CT. Ocean Eng. 301, 117492. https://doi.org/10.1016/j.oceaneng.2024.117492.

Zhao, Y.J., Hu, W., Dou, X.F., et al., 2024a. Experimental investigation on the geological responses and production behaviors of natural gas hydrate-bearing sediments under various hydrate saturations and depressurization strategies. Appl. Energy 347, 123952. https://doi.org/10.1016/j.apenergy.2024.123952.

Zhao, Y.J., Liu, Z.C., Li, Y.F., et al., 2024b. Subsidence characteristics of hydrate-bearing sediments during depressurization: insights from experimental and discrete element method simulations. Energy Fuels 38 (17), 16202–16217. https://doi.org/10.1021/acs.energyfuels.4c01534.

Zhao, Z., Shou, Y.D., Zhou, X.P., 2023. Digital assessment of phase changes and heat transfer for hydrates in microstructures using X-ray CT imaging. Geoenergy Sci. Eng. 229, 212084. https://doi.org/10.1016/j.geoen.2023.212084.

Zhu, H.X., Xu, T.F., Xin, X., et al., 2022. Numerical investigation of natural gas hydrate production performance via a more realistic three−dimensional model. J. Nat. Gas Sci. Eng. 107 (Suppl. C), 104793. https://doi.org/10.1016/j.jngse.2022.104793.

Zyrianova, M., Collett, T., Boswell, R., 2024. Characterization of the structural-stratigraphic and reservoir controls on the occurrence of gas hydrates in the Eileen Gas Hydrate trend, Alaska North Slope. J. Mar. Sci. Eng. 12 (3), 472. https://doi.org/10.3390/jmse12030472.